AD-A108 212 SCIENCE APPLICATIONS INC MCLEAN VA F/G 20/4
STATISTICAL MODELING OF SHEAR IN THE UPPER OCEAN.(U)
MAR 81 G T HEBENSTREIT, W J GRABOWSKI N00014-81-C-0084
UNCLASSIFIED SAI-82-382-WA NL

END
DATE FILMED
4-82
DTIC

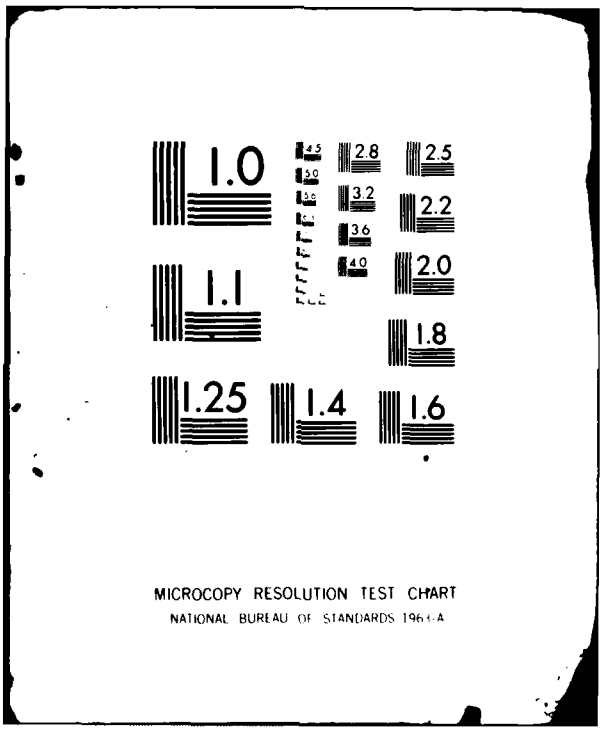
1.0
1.1
1.25
1.4
1.6
1.8
2.0
2.2
2.5
2.8
3.2
3.6
4.0
4.5
5.0
5.6
MICROCOPY RESOLUTION TEST CHART
NATIONAL BUREAU OF STANDARDS 1963-A

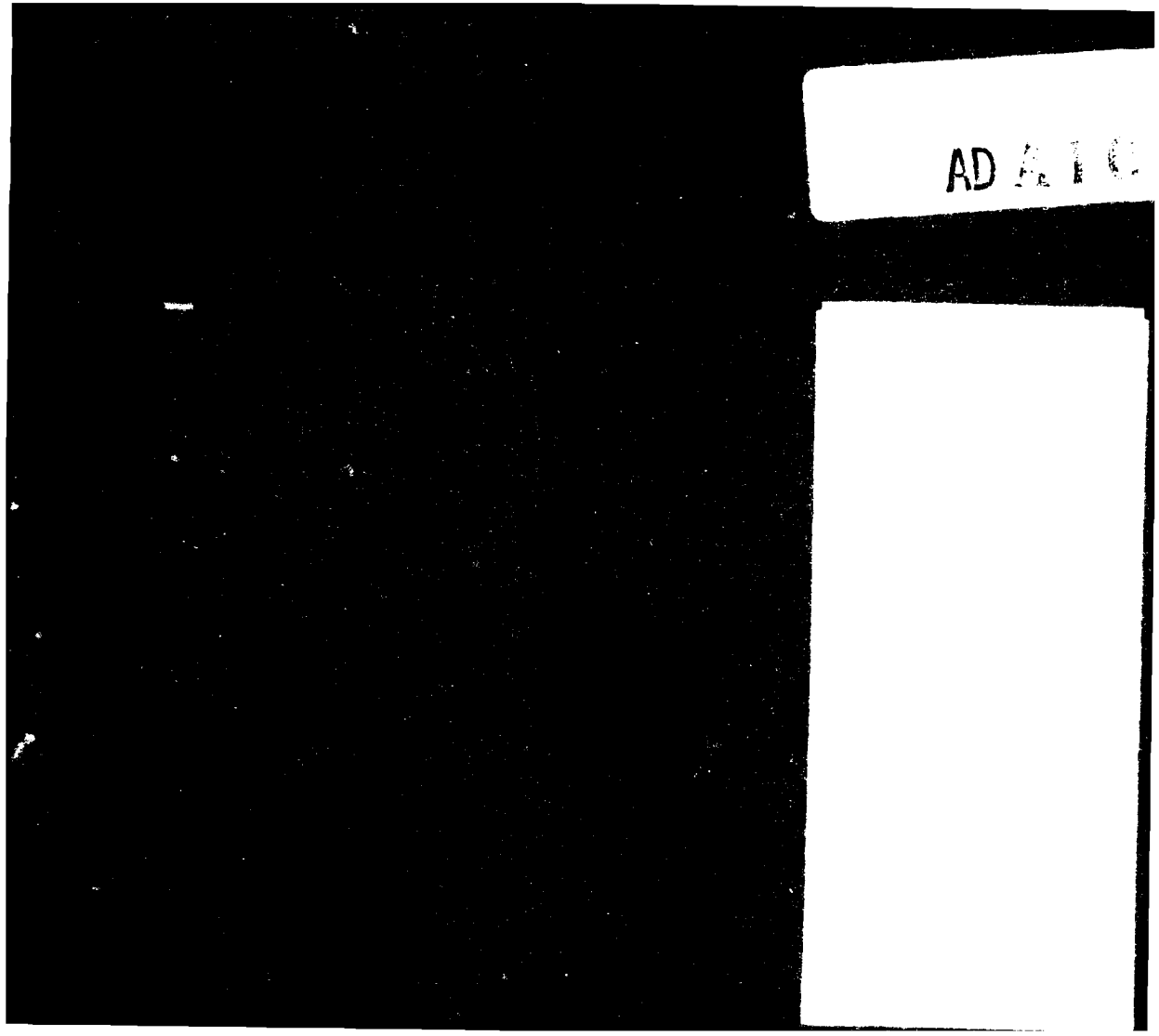
AD

STATISTICAL MODELING OF SHEAR IN THE UPPER OCEAN

SAI-82-382-WA

SAI
ATLANTA • ANN ARBOR • BOSTON • CHICAGO • CLEVELAND • DENVER • HUNTSVILLE • LA JOLLA
LITTLE ROCK • LOS ANGELES • SAN FRANCISCO • SANTA BARBARA • TUCSON • WASHINGTON

STATISTICAL MODELING OF SHEAR IN THE UPPER OCEAN

SAI-82-382-WA

1 March 1981

Prepared by:
Gerald T. Hebenstreit
Walt Grabowski
Ocean Physics Division

Prepared for:
Ocean Measurements Program
Contract N00014-81-C-0084
Naval Ocean Research and Development Activity
NSTL Station
Bay St. Louis, MS

SCIENCE APPLICATIONS, INC.

P.O. Box 1303
1710 Goodridge Drive
McLean, Virginia 22102
(703) 821-4300

UNCLASSIFIED

SECURITY CLASSIFICATION OF THIS PAGE (When Data Entered)

REPORT DOCUMENTATION PAGE		READ INSTRUCTIONS BEFORE COMPLETING FORM
1. REPORT NUMBER SAI-82-382-WA	2. GOVT ACCESSION NO. AD-A108 223	3. RECIPIENT'S CATALOG NUMBER
4. TITLE (and Subtitle) Statistical Modeling of Shear in the Upper Ocean		5. TYPE OF REPORT & PERIOD COVERED Technical 1/11/80 - 3/24/81
		6. PERFORMING ORG. REPORT NUMBER SAI-82-382-WA
7. AUTHOR(s) Gerald T. Hebenstreit Walter J. Grabowski		8. CONTRACT OR GRANT NUMBER(s) N00014-81-C-0084
9. PERFORMING ORGANIZATION NAME AND ADDRESS Science Applications, Inc. 1710 Goodridge Drive McLean, VA 22102		10. PROGRAM ELEMENT, PROJECT, TASK AREA & WORK UNIT NUMBERS
11. CONTROLLING OFFICE NAME AND ADDRESS Office of Naval Research 800 N. Quincy Street Arlington, VA 22217		12. REPORT DATE 1 March 1981 13. NUMBER OF PAGES 71
14. MONITORING AGENCY NAME & ADDRESS (if different from Controlling Office) Scientific Officer Ocean Exploratory Development Office Naval Ocean Research and Development Activity NSTL Station, Bay St. Louis, MS 34529 ATTN: Dr. E. M. Stanley, NORDA, Code 500		15. SECURITY CLASS. (of this report) UNCLASSIFIED 15a. DECLASSIFICATION/DOWNGRADING SCHEDULE N/A

16. DISTRIBUTION STATEMENT (of this Report)

[redacted]

17. DISTRIBUTION STATEMENT (of the abstract entered in Block 20, if different from Report)

18. SUPPLEMENTARY NOTES

19. KEY WORDS (Continue on reverse side if necessary and identify by block number)

Shear
Statistical Modeling
Upper Ocean Shear
Velocity Profiles
YVETTE
Hypothesis Testing

20. ABSTRACT (Continue on reverse side if necessary and identify by block number)

Analysis of upper ocean shear profiles obtained with a free-fall sampling instrument (YVETTE) indicated that, within specific depth regimes and for specified vertical differencing intervals, values of shear-squared might be distributed according to a χ^2 probability distribution. An analysis based on several assumptions about the shear field produced a model which showed that a χ^2 distribution was physically reasonable. Statistical tests on the profiles led to acceptance of the hypothesis that S^2

DD FORM 1 JAN 73 1473 EDITION OF 1 NOV 65 IS OBSOLETE
S/N 0102-LF-014-6601

UNCLASSIFIED

SECURITY CLASSIFICATION OF THIS PAGE (When Data Entered)

follows a χ^2 distribution with a variance derived from the mean-square shear in the regime. Further statistical tests showed that the necessary assumptions about the horizontal shear components were statistically reasonable as well as physically reasonable. A trial prediction using a simple linear relationship between mean Brunt-Väisälä frequency in a regime and mean shear-squared, based on a 2m separation, in the regime showed the χ^2 model to be a potentially useful tool for area characterizations.

TABLE OF CONTENTS

LIST OF FIGURES

LIST OF FIGURES (Continued)

LIST OF FIGURES (Continued)

LIST OF TABLES

Section 1
INTRODUCTION

The objective of this study is to determine if a basis can be established for a statistical model of the distribution of vertical shear (vertical gradient of horizontal velocity) in the upper ocean. We have approached this problem in three stages:

- Define as our basic descriptor the probability distribution of shear squared;
- Determine how well this observed probability distribution can be described by a known analytic probability distribution;
- Test the assumptions which would have to be satisfied to ensure that the observed samples do, indeed, come from the known distribution.

In order to examine these questions, we have analyzed vertical profiles of horizontal velocity in the upper ocean provided by David Evans of the University of Rhode Island. The data were collected by a sensor system called YVETTE.

In Section 2 we briefly describe the YVETTE data. A more detailed description is given by Lambert et al. (1980). We also describe the processing which we applied

to the YVETTE profiles and the general characteristics of the data. In Section 3 we derive an analytic model for the probability distribution of mean-square shear. This model leads us to speculate that the occurrence of shear-squared values in various depth regimes follows a χ^2 probability distribution. In Section 4 we test this hypothesis statistically in two ways. In one we compare directly the observed shear-squared distributions with suitable χ^2-distributions to assess the acceptability of the hypothesis, while in the other we test how well the statistical (as opposed to physical) assumptions required for a χ^2-distribution are satisfied by the data. In Section 5 we describe an attempt to implement the χ^2 model by making use of a possible relationship between $\overline{N^2}$ and $\overline{S^2}$ proposed by Patterson et al.(1981) in a companion SAI report. We discuss the utility of this model and make recommendations for further improvements.

Section 2

YVETTE VELOCITY PROFILES - OVERVIEW

2.1 YVETTE STATIONS

The data on which our analysis is based were obtained by David Evans of the University of Rhode Island in 1975 and 1977 with a vertical profiling instrument, YVETTE. At the time these profiles were measured YVETTE was a four-meter-long tube equipped with Neil Brown conductivity, temperature, and depth (CTD) sensors as well as an orthogonal pair of acoustic current meters. A detailed description of YVETTE is provided by Evans et al. (1979). When deployed, the probe fell freely through the water column at a rate of 25 cm s^{-1}. The water temperature, conductivity, two orthogonal components of horizontal velocity relative to the probe housing, and the orientation of the instrument relative to the earth's magnetic field were recorded internally on magnetic cassette tape. The sensors were sampled at a rate of 2.5 times per second to yield a vertical sampling interval of approximately 10 cm. The CTD sensors had a resolution of 0.001 mmho cm^{-1}, 0.0005°C, and 0.05 dbar, respectively. The acoustic current meters had a sensitivity of 0.05 cm s^{-1} and the compass could resolve orientation to within 3°.

The data set provided to us was filtered to remove variations on vertical scales less than 2 m. The velocity

profiles were corrected for horizontal drag effects imposed on the system housing by the large-scale vertical shear. A description of this processing is contained in Lambert et al. (1980). The resulting data set should, in principle, include velocity structure resolved over vertical scales between 2 m and 100 m.

The data set consists of fifteen stations, fourteen in various parts of the North Atlantic Ocean and one in the Pacific Ocean. The position, date, and time of these profiles are listed in Table 2.1. Figure 2.1 shows the profile locations.

2.2 VELOCITY DATA PROCESSING

The profiles of horizontal velocity obtained from Evans consisted of values spaced irregularly in the vertical (pressure) direction with a typical spacing of one meter. Our first step in analyzing shear values was to interpolate the irregularly spaced values to a profile of values at regular intervals. We did this with a cubic-spline interpolation to produce values of u and v at intervals of 1m. We then performed numerical differentiations over specified separations. We considered separations, Δz, of 2, 4, 8 and 16 m in this study.

We define shear-squared at depth z as the squared magnitude of the difference between the horizontal velocity vector $\underline{v}$ at depth $z + \frac{1}{2}\Delta z$ and $z - \frac{1}{2}\Delta z$, normalized by $(\Delta z)^2$. That is

$$S^2(z;\Delta z) = |\underline{v}(z+\tfrac{1}{2}\Delta z) - \underline{v}(z-\tfrac{1}{2}\Delta z)|^2(\Delta z)^{-2} \quad ,$$
$$= (\Delta_z u)^2 + (\Delta_z v)^2 \quad , \qquad (2.1)$$

Table 2.1

YVETTE STATIONS[1]

Station Number	Time (GMT)	Date	Latitude (N)	Longitude (W)	Comment
5	1942	5 Nov. 75	32°19'	64°34'	Near Bermuda
8	0225	8 Nov. 75	35°00'	66°30'	Sargasso Sea
9	1219	"	"	"	"
10	1814	9 Nov. 75	38°09'	69°06'	Gulf Stream
11	0036	10 Nov. 75	38°05'	69°03'	"
12	1312	"	38°15'	69°07'	"
18	—	7 May 77	22°47'	70°43'	Edge of thermocline eddy
21	—	9 May 77	22°27'	70°57'	Center of thermocline eddy
23	—	16 May 77	36°24'	67°36'	Outer part of GSR[2]
24	—	"	36°20'	67°44'	Midway along radius of GSR
25	—	17 May 77	36°09'	67°53'	Near center of GSR
NOR 1	—	1973	—	—	Norwegian Fjord
NOR 4	—	"	—	—	"
NOR 6	—	"	—	—	Norwegian Coastal Current
EPOCS[3]6	—	July 79	0°03'	109°57'	Data start just below EUC[4]

1 Adapted from Lambert et al. (1980)

2 Gulf Stream Ring

3 Equatorial Pacific Ocean Climate Study

4 Equatorial Undercurrent

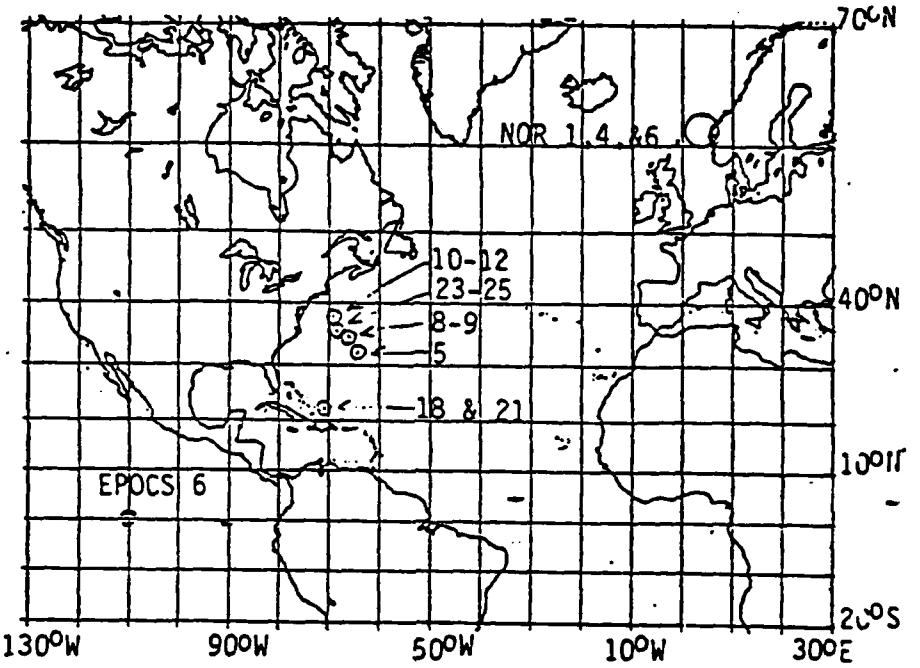

Figure 2.1 Positions of YVETTE Stations

where u and v refer to velocity components in the east-west and north-south directions and

$$\Delta_z u = \left[u(z+\tfrac{1}{2}\Delta z) - u(z-\tfrac{1}{2}\Delta z)\right]\Delta z^{-1} \qquad (2.2)$$

with a similar expression for $\Delta_z v$. Since we used non-overlapping differences, we obtained fewer shear estimates as we increased the spacing.

Once the $\Delta_z u$ and $\Delta_z v$ values were calculated, we calculated the depth average of each profile, defined as

$$\overline{\Delta_z u} = \frac{1}{N}\sum_{i=1}^{N} \Delta_z u(z_i) \qquad (2.3)$$

with a similar expression for $\overline{\Delta_z v}$. By subtracting the average from the individual values we obtained modified data $\Delta_z u'$ and $\Delta_z v'$:

$$\Delta_z u'(z_i) = \Delta_z u(z_i) - \overline{\Delta_z u} \quad . \qquad (2.4)$$

In this way we removed any linear trend which might have occurred in the data.

The S^2 values used in this study are defined as

$$S^2 = (\Delta_z u')^2 + (\Delta_z v')^2 \quad . \qquad (2.5)$$

2.3 SAMPLE STATION - YVETTE 08

The first station we analyzed was YVETTE 08 from the Sargasso Sea. Figures 2.2 and 2.3 show plots of the data received from URI for this station.* Note the presence of an upper isopycnal layer, a sharp pycnocline below that, and a region of less steep but still increasing density below that. We have divided the profiles for this station into three regimes: the surface mixed layer (ML), the upper thermocline (UT), and the deep layer (DL). The dotted lines in the figures denote rather subjective boundaries between these layers. The values of $\Delta_z u$ and $\Delta_z v$ tend to be highest in the upper-thermocline region where the Brunt-Väisälä frequency is highest and lower in the surface mixed and deep layers. This apparent correlation is explored in detail by Patterson et al. (1981). We will return to its implication later in this document.

All of the YVETTE profiles were divided into subprofiles in this manner, using divisions established by Patterson et al. (1981) on the basis of changes in Brunt-Väisälä frequency. We have retained their definitions of the layers without modification.

---

* The profiles shown in these figures were taken directly from data provided by Evans. The actual data points are located at irregularly spaced depths as mentioned earlier.

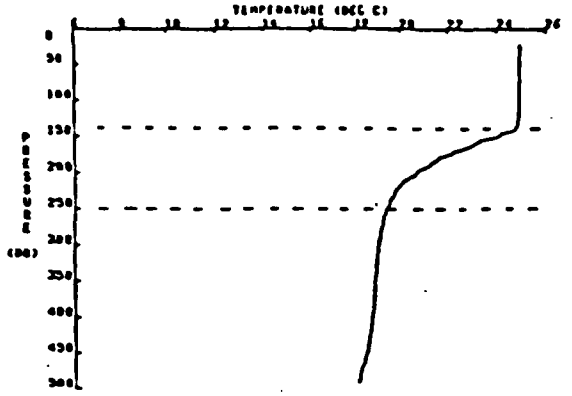

(a) Temperature

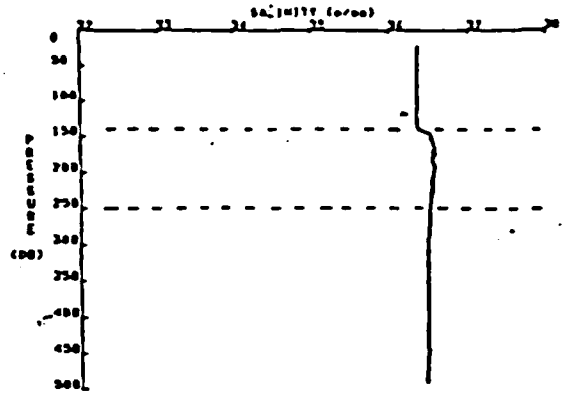

(b) Salinity

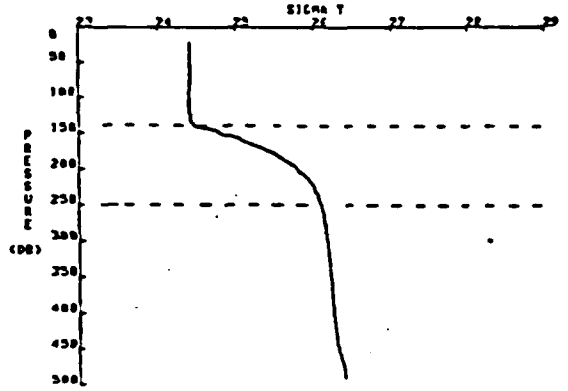

(c) Density

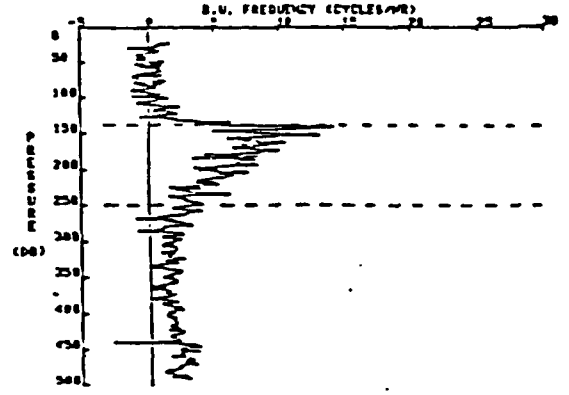

(d) Brunt-Väisälä Frequency

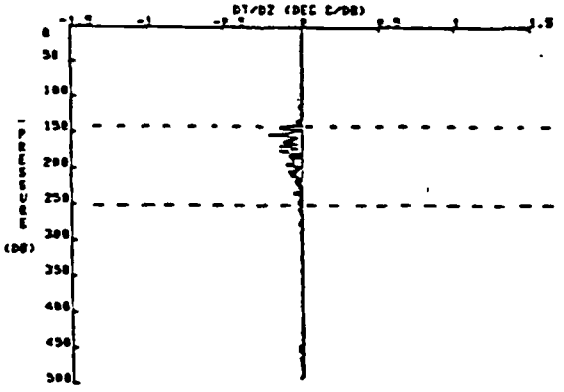

Temperature Gradient

Figure 2.2 Profiles from YVETTE station 8 occupied on 8 November 1975 at 35°00'N, 66°30'W (Sargasso Sea). The profiles can be divided into stratification regimes as indicated by the dotted lines at 135 and 250 dbars.

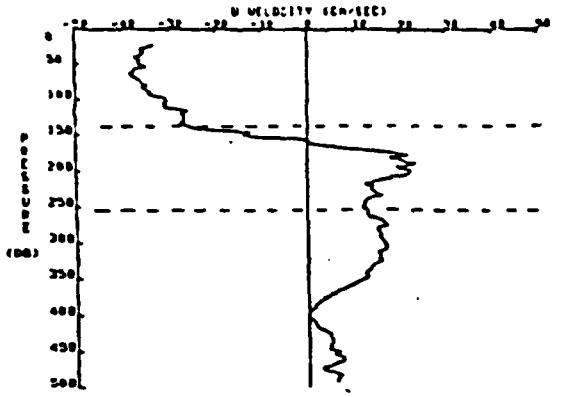

(a) East Velocity Component

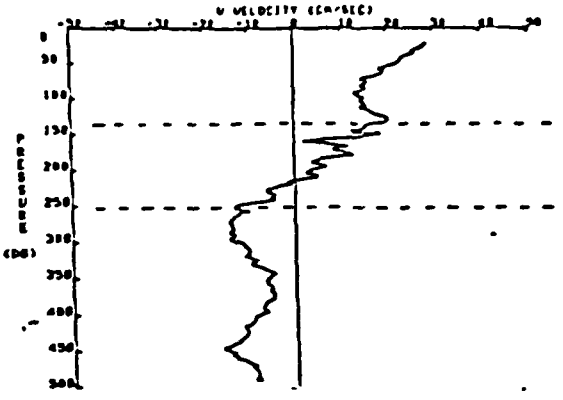

(b) North Velocity Component

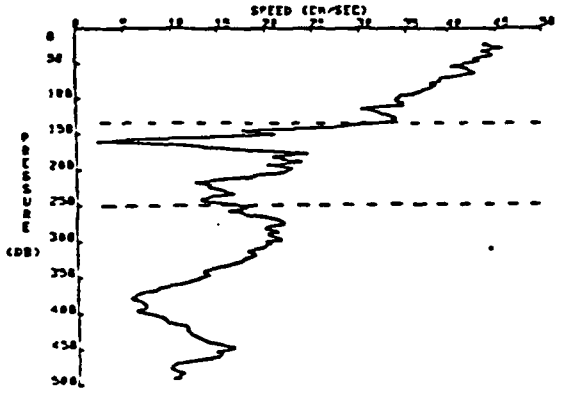

(c) Current Speed

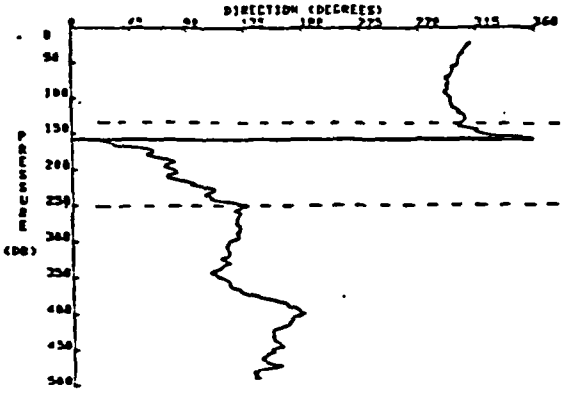

(d) Current Direction

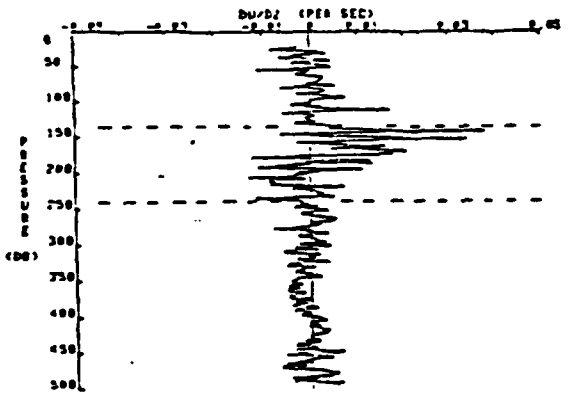

(e) $\Delta_z u$

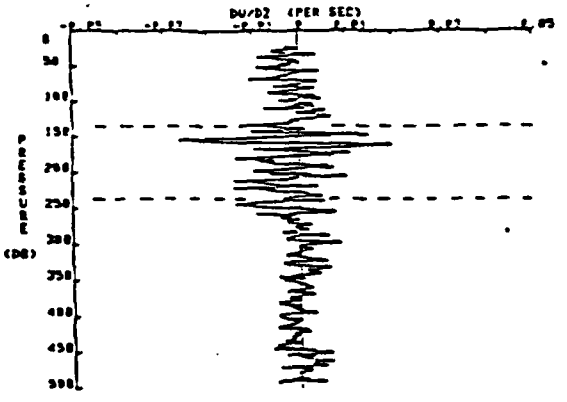

(f) $\Delta_z v$

Figure 2.3 Profiles of the (a) east and (b) north component of velocity, the (c) magnitude and (d) direction of the horizontal velocity vector, and the vertical gradient of the (e) east and (f) north component of velocity for YVETTE station 8 in the Sargasso Sea. The dotted lines are at 135 and 250 dbars.

Shear-squared profiles which we computed by applying (2.5) to the interpolated velocity profiles from this station are shown in Figure 2.4. The calculations with 2, 4, 8 and 16 m spacings are all presented.

In order to examine the distribution of values of S^2 we divided the range from $S^2 = 0$ to $S^2 =$ maximum in each profile segment into equi-width bins such that the range would be subdivided into 30-40 bins. We then generated histograms of the number of values falling into each bin. These were expressed as the fraction of the total number of values in each profile segment. Histograms for the three depth regimes of YVETTE 08 are shown in Figure 2.5a-c. The histograms indicate that the data display a strong preference for low values of S^2 compared to the total range of observed values. The coarse quality of the histograms for 8 m and 16 m separations is due to the small number of S^2 values in the samples.

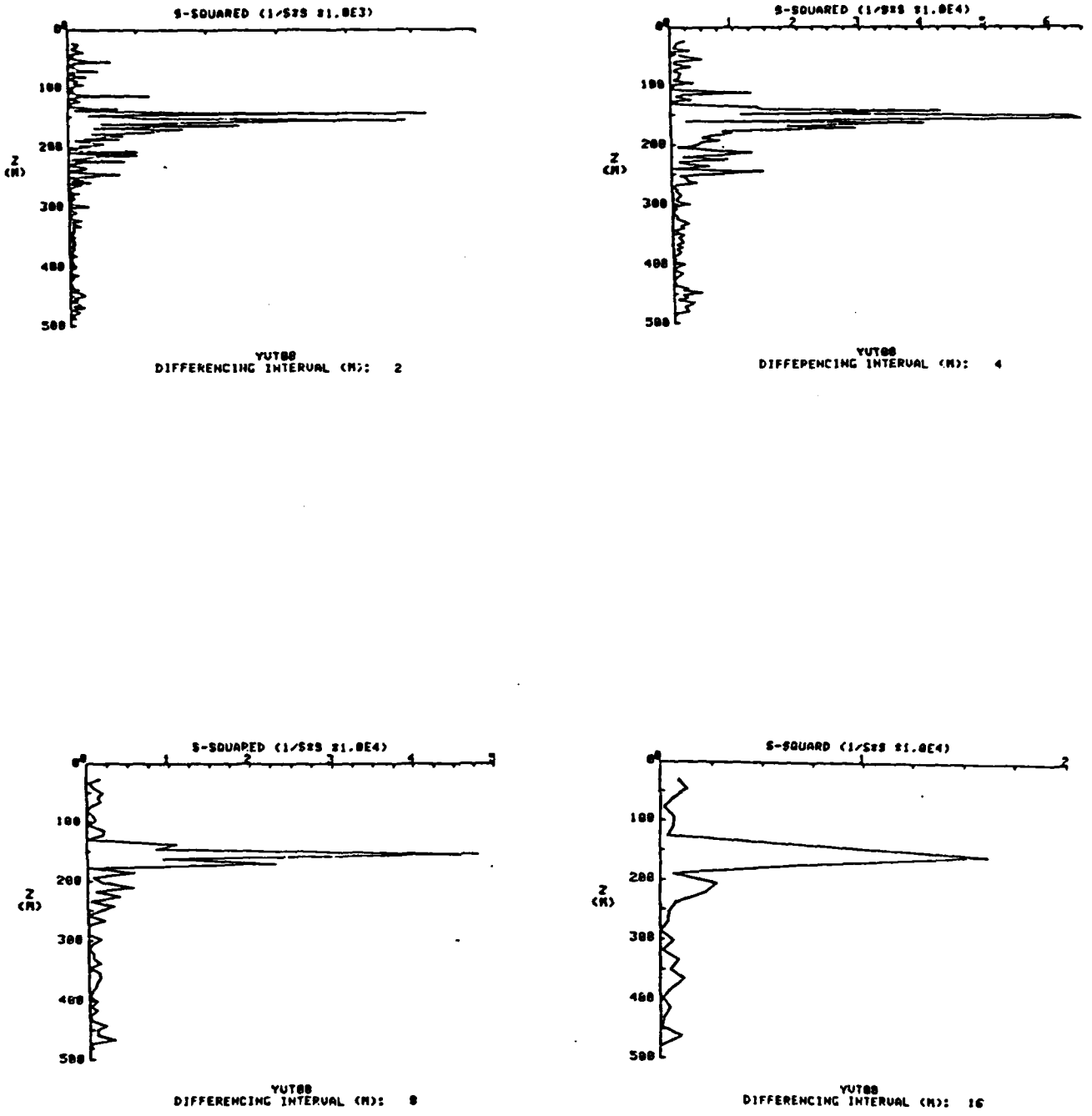

Figure 2.4 Shear-squared profiles for spacings, Δz, of 2, 4, 8 and 16 m from interpolated YVETTE 08 data.

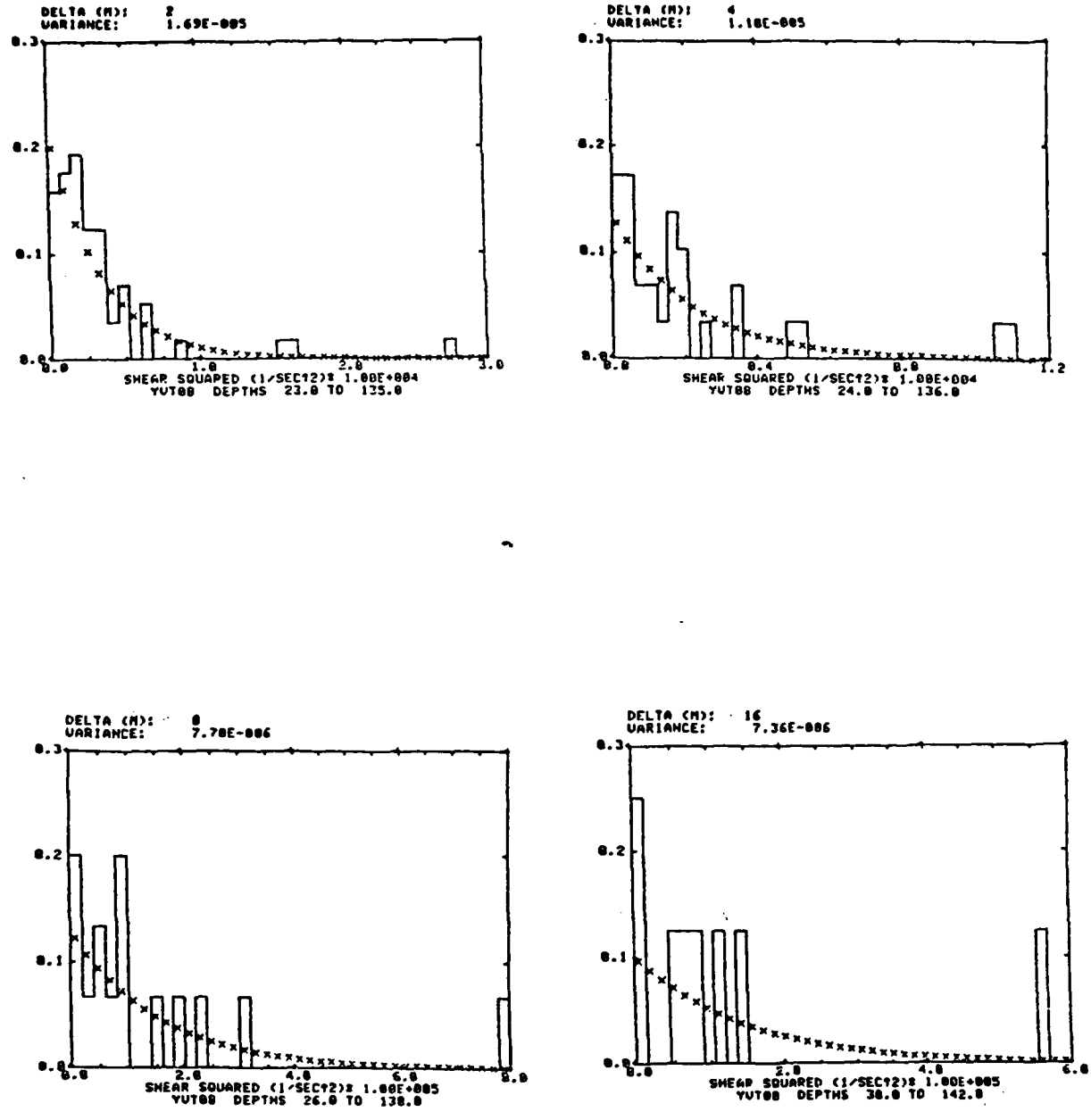

Figure 2.5a Frequency of occurrence histograms of shear squared with 2, 4, 8 and 16 m spacings from YVETTE 08. x's represent a χ^2 probability density with variance calculated from the sample.

(a) Mixed layer

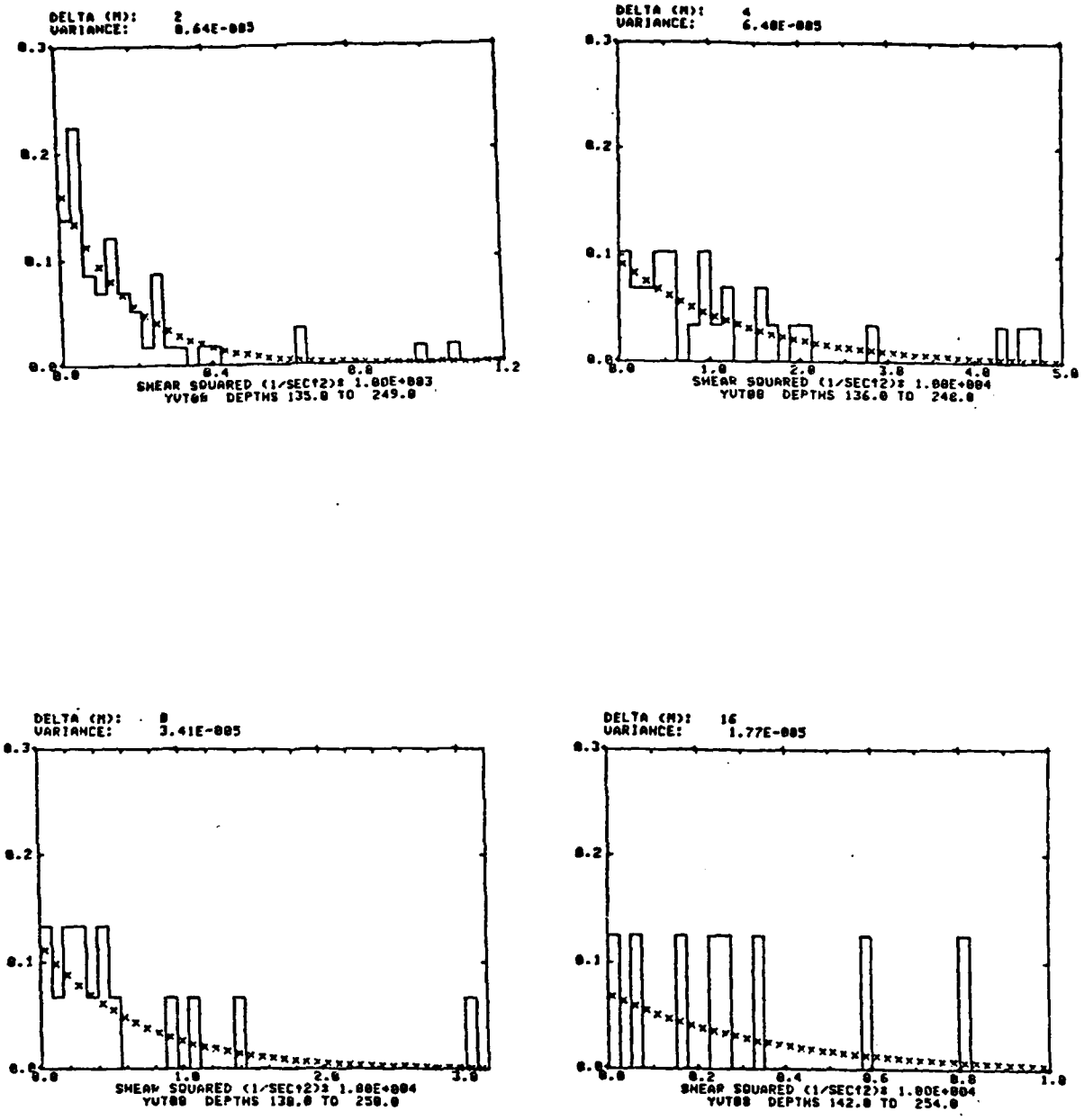

Figure 2.5b Frequency of occurrence histograms of shear squared with 2, 4, 8 and 16 m spacings from YVETTE 08. x's represent a χ^2 probability density with variance calculated from the sample.

(b) Upper thermocline

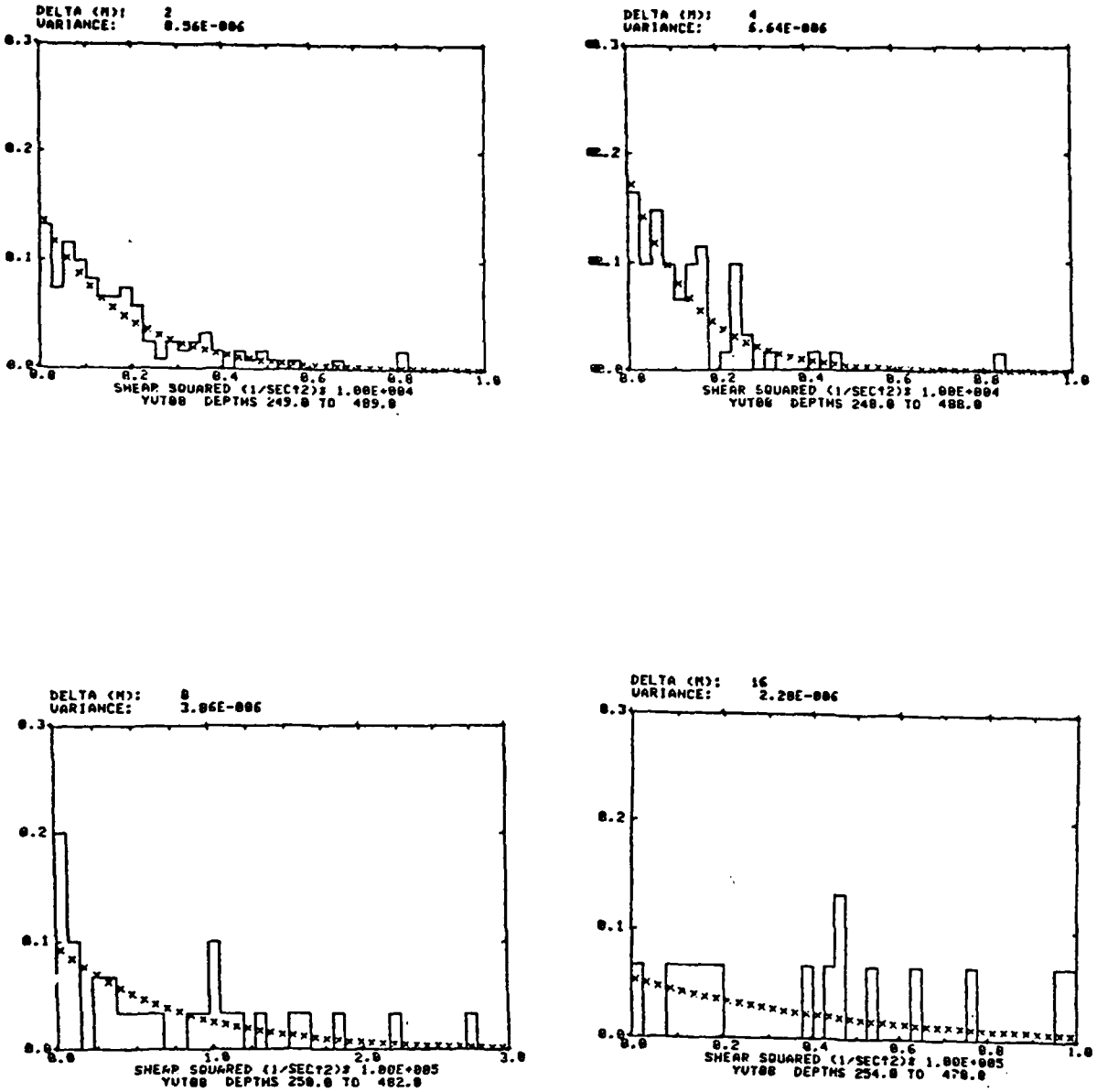

Figure 2.5c Frequency of occurrence histograms of shear squared with 2, 4, 8 and 16 m spacings from YVETTE 08. x's represent a χ^2 probability density with variance calculated from the sample.

(c) Deep layer

Section 3
SHEAR DISTRIBUTION MODEL

It is possible to derive a model for a shear probability density function $B(S^2; \Delta z)$ with the application of a few assumptions about the statistical properties of the shear field. The assumptions are simple (but not trivial). In this section we derive such a model and in Section 4 we apply it to the data.

The basic idea was developed by Bretherton (1969). He supposed that only one component $\Delta_z u$ of the vertical velocity difference was significant and that this difference represented the sum of the vertical gradients associated with a large number of linearly independent, random internal waves. Thus, by the central-limit theorem, $\Delta_z u$ is normally distributed, and

$$B(\Delta_z u; \Delta z) = (\sigma\sqrt{2\pi})^{-1} \exp[-\tfrac{1}{2}(\Delta_z u)^2 \sigma^{-2}] \quad (3.1a)$$

where the variance

$$\sigma^2 = \langle(\Delta_z u)^2\rangle \quad (3.1b)$$

and the braces indicate ensemble averaging (or over a very large number of independent samples).

The density function is defined in the usual way with

$$\text{Prob}\,(\lambda_o \le \lambda \le \lambda_o + d\lambda) = B(\lambda_o; \Delta z)\, d\lambda\,. \quad (3.2)$$

The probability density function for $S_1^2(\Delta z)$ (where subscripts 1 refers to a single component of velocity) is given by the chi-square density with one degree of freedom:

$$B(S_1^2;\Delta z) = [\sigma \sqrt{2}\, S_1\, \Gamma(\tfrac{1}{2})]^{-1} \exp(-\tfrac{1}{2}S_1^2\sigma^{-2}).^* \qquad (3.3)$$

We extend the analysis to allow two velocity components to contribute to the mean-square shear. We assume that the velocity difference vector $(\Delta_z u,\ \Delta_z v)$ represents the vector sum of velocity differences associated with a large number of linearly independent random phenomena. Then the Multidimensional Central Limit Theorem (Loeve, 1960) implies that the two-dimensional probability density function $B(\Delta_z u, \Delta_z v; \Delta z)$ of the vector approaches a two-dimensional normal distribution. Thus,

$$B(\Delta_z u,\Delta_z v;\Delta z) = (2\pi\sigma^2\sqrt{1-r^2})^{-1} \times \exp\left\{-\tfrac{1}{2}(1-r^2)\sigma^{-2}\left[(\Delta_z u)^2 + (\Delta_z v)^2 - 2r\,\Delta_z u\,\Delta_z v\right]\right\}, \qquad (3.4)$$

where σ^2 is as defined in (3.1b) and r is the covariance

$$r = \langle \Delta_z u\ \Delta_z v \rangle\ \sigma^{-2}$$

We assume that the wave field is isotropic. Therefore.

$$r = 0 \qquad (3.5)$$

---

* $\Gamma(\tfrac{1}{2})$ is approximately 1.772 so that the quantity in the brackets is approximately $2.5\sigma\ S_1$.

and

$$\langle \Delta_z u \Delta_z v \rangle = 0 \ .$$

Each individual probability density is given by (3.1) so that the velocity components are normally distributed. The separability of the probability densities is a definition of statistical independence. Hence the velocity difference components $\Delta_z u$ and $\Delta_z v$ are not only uncorrelated (3.5) but statistically independent.

It is now straightforward to obtain the probability density function of S^2. The sum of the squares of n normally distributed, independent random variables with identical distributions has a chi-square probability density, with n degrees of freedom (Papoulis, 1965). Thus S^2 has a 2-degree-of-freedom density given by

$$B(S^2;\Delta z) = (2\sigma^2)^{-1} \exp\left(-\tfrac{1}{2}S^2\sigma^{-2}\right) \qquad (3.6a)$$

for $S^2 > 0$. The density function in (3.6) is not sharply peaked for small values of its argument whereas that in (3.3) is. At large values of its argument, the value given by (3.6a) is larger than given by (3.3).

We can integrate (3.6a) to show that the expected value of S^2 is

$$\begin{aligned} \mu_{S^2} &\equiv \langle S^2 \rangle \\ &= 2\sigma^2 \end{aligned} \qquad (3.6b)$$

and that the variance of S^2 is

$$\sigma^2_{S^2} \equiv \langle S^2 - \langle S^2 \rangle \rangle = 4\sigma^4 \qquad (3.6c)$$

We propose that (3.6a) be tested as a model for the probability density of mean square shear. Instead of $B(S^2;\Delta z)$ a more useful statistical description is given by the probability distribution function

$$\chi^2(S^2;\Delta z) \equiv \int_{-\infty}^{S^2} B(S^2;\Delta z)dS^2 \tag{3.7}$$

so that

$$\text{Prob} \quad (S^2 \leq S_o^2) = \chi^2(S_o^2;\Delta z).$$

From (3.6) and (3.7)

$$\chi^2(S^2;\Delta z) = 1-\exp(-\tfrac{1}{2}S^2\sigma^{-2}). \tag{3.8}$$

Figure 2.5 referred to earlier shows the S^2 histogram computed from data from YVETTE 08 data. Superposed on that figure are $B(S^2;\Delta z)$ density functions given by (3.6). In theory, the component variance used in the χ^2 probability is given by

$$\sigma^2 = \sigma_x^2 = \sigma_y^2 \quad .$$

That is, σ_x^2 and σ_y^2 (assumed identical) are the variances of the population distributions of the shear components. In practical terms, however, we used the estimate $\hat{\sigma}^2$ given by

$$\hat{\sigma}^2 = \tfrac{1}{2}(\hat{\sigma}_x^2 + \hat{\sigma}_y^2) \quad . \tag{3.9}$$

the average of the estimates of the variances of the two components of the sample, since the two component variances are not exactly equal.

The definitions of $\hat{\sigma}_x^2$ and $\hat{\sigma}_y^2$ lead to

$$\hat{\sigma}^2 = \tfrac{1}{2}\left[\frac{1}{N-1}\sum_{i=1}^{N}(\Delta u_i/\Delta z)^2 + \frac{1}{N-1}\sum_{i=1}^{N}(\Delta v_i/\Delta z)^2\right] \tag{3.10}$$

where N is the number of samples in the depth regime. Note that the means of the shear components have been removed (i.e., Δu_i are equivalent to $\Delta u_i'$ of 2.4).

Combining (3.10) and (2.5) leads to:

$$\hat{\sigma}^2 = \tfrac{1}{2}\frac{1}{N-1}\sum_{i=1}^{N}\left[(\Delta u_i/\Delta z)^2 + (\Delta v_i/\Delta z)^2\right]$$

$$= \tfrac{1}{2}\frac{1}{N-1}\sum_{i=1}^{N} s_i^2.$$

$$= \tfrac{1}{2}\frac{N}{N-1}\hat{\mu}_{s^2} \tag{3.11}$$

Section 4
SHEAR DISTRIBUTION ANALYSIS

In Section 3 we derived a χ^2 model for the distribution of upper-ocean mean-square shear. In this section we test the applicability of that model. Our approach makes use of the tools of hypothesis testing, in particular, a Kolmogorov-Smirnov "goodness-of-fit" test.

We characterize the appropriateness of the model in terms of the critical level of significance (defined below), which we can attach to the hypothesis that the S^2 values are drawn from a population which has a χ^2 distribution. We estimate the population variance as the variance of the sample. A goodness-of-fit test for a hypothetical distribution in which some significant aspect of the hypothesized distribution is calculated from the sample is a "conservative" test. This means that the test results are biased toward higher critical levels of significance.*

We also describe the results of (nonconservative) statistical tests performed on the data to ascertain whether the conditions on the velocity field necessary for a χ^2 shear distribution were met. We applied a Cox-Stuart trend test for randomness of the samples of the individual

---

* Conservative here implies that since the results are biased toward higher apparent levels of significance we are less likely to make a decision to reject a stated null hypothesis.

components $\Delta_z u$ and $\Delta_z v$; a Lilliefors test for normality of the components; a χ^2 test for mutual independence of the components; and a Smirnov test for identical distribution functions of the two components.

A review of hypothesis testing is presented in Appendix A.

4.1 GOODNESS-OF-FIT TESTS FOR SHEAR

4.1.1 Critical Levels

In order to quantify the degree to which shear distributions for each profile segment can be represented by a χ^2 distribution (conservatively, with variance set to the sample variance), we applied the Kolmogorov goodness-of-fit test. The sole assumption required by this test is that the values of S^2 be random.

The test consists of comparing the observed probability distribution $G(S^2)$, calculated from the sample, to the hypothesized distribution $\chi^2(S^2)$ with σ^2 estimated by $\hat{\sigma}^2$. We obtained the observed probability distribution simply by ordering S^2 values from low to high (index j) and calculating the cumulative sum of values less than or equal to a given value:

$$G(S_i^2) = \frac{1}{N} \sum_{j=1}^{N} H(x_i - x_j) \quad \text{where} \quad H=1,\ x_j \leq x_i \ . \qquad =0,\ x_j > x_i \ . \qquad (4.1)$$

The corresponding hypothetical probability is $\chi^2(S_i^2;\hat{\sigma}^2)$. The test statistic is the maximum difference between these two functions at any S_i:

$$\underline{T} = \sup_{S_i^2} \left| G(S_i^2) - \chi^2(S_i^2) \right| \qquad (4.2)$$

where "sup" refers to the maximum value. The empirical $\underline{T}$ is then compared to tables of quantiles of $\underline{T}$ predicted from a postulated $\underline{T}$ distribution. Table B.1 shows the quantiles of the Kolmogorov test statistic. The quantity n is the number of points in the sample and $\rho\,(=1-\alpha)$ is the "confidence level".

We define let $\underline{T}_1$ be the test statistic associated with one individual test. The first quantile value higher than $\underline{T}_1$ is associated with the approximate critical confidence and significance levels, $\hat{\rho}$ and $\hat{\alpha}$. For example, if the value of $\underline{T}_1$, based on a sample of 30 points, were 0.200, then $0.8 < \hat{\rho} < 0.9$ and $0.2 > \hat{\alpha} > 0.1$. On the other hand, if T_1 for the same case were 0.288, then $0.98 < \hat{\rho} < 0.99$ and $0.02 > \hat{\alpha} > 0.01$.*

Figure 4.1a-c shows the graphical comparison between the observed and the calculated χ^2 cumulative probabilities for YVETTE 08. The statistic $\underline{T}_1$ is the greatest separation between the two functions along a vertical line corresponding to one of the observed values of S^2. In all the cases depicted $\hat{\alpha}$ was at least 0.20. Thus the model falls within the 80% confidence interval of the observed distribution.

---

* The quantity $\hat{\rho} = 1 - \hat{\alpha}$ defines the confidence level around the empirical distribution at which the model distribution falls. A value of $0.1 < \hat{\alpha} < 0.2$ implies that the model falls within the 80 to 90% confidence intervals.

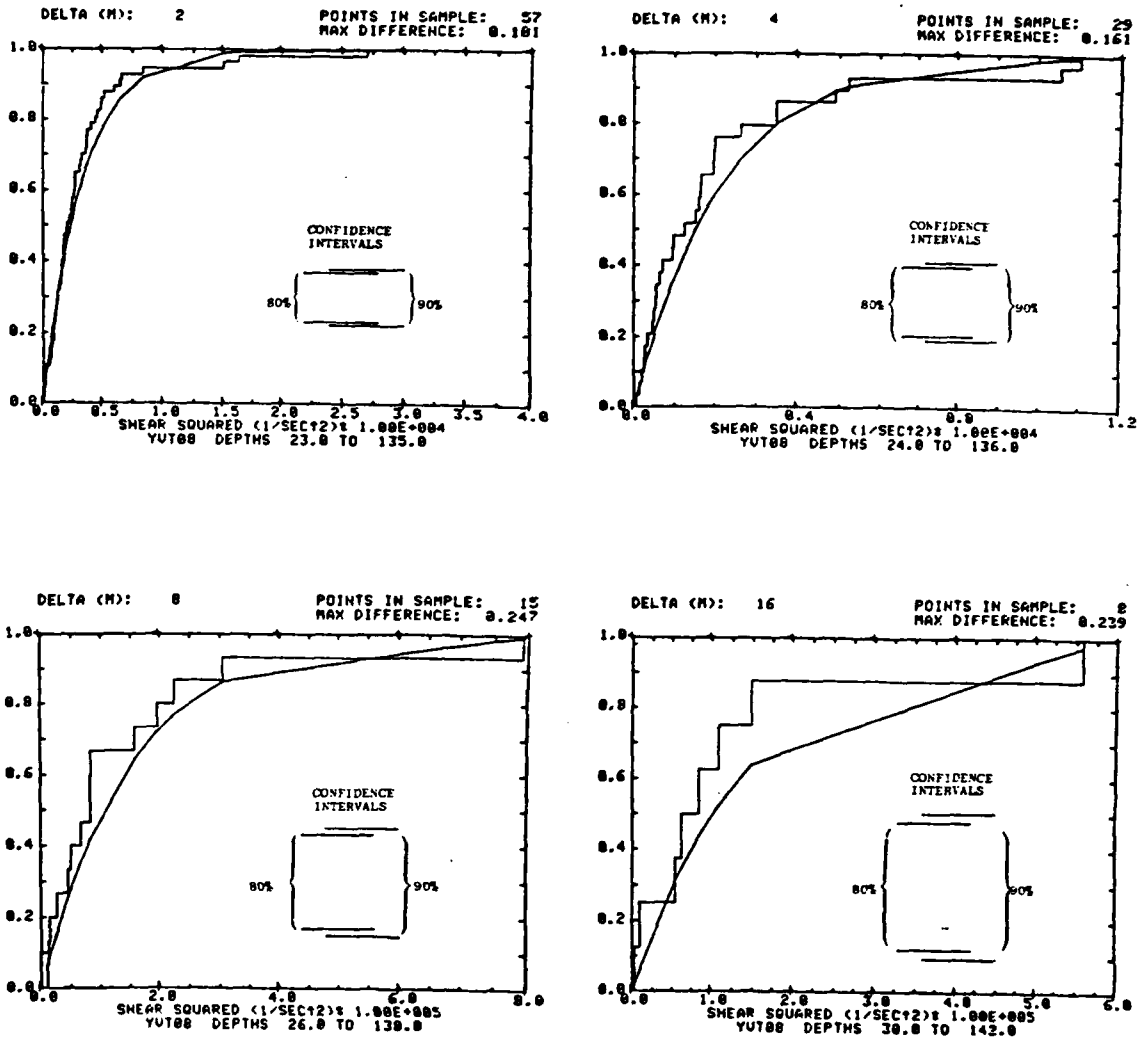

Figure 4.2a Graphical comparison between observed probability of S^2 (step function) and hypothesized χ^2-distribution (smooth function) based on the ML of YVETTE 08. Test statistic is the maximum vertical distance between curves.

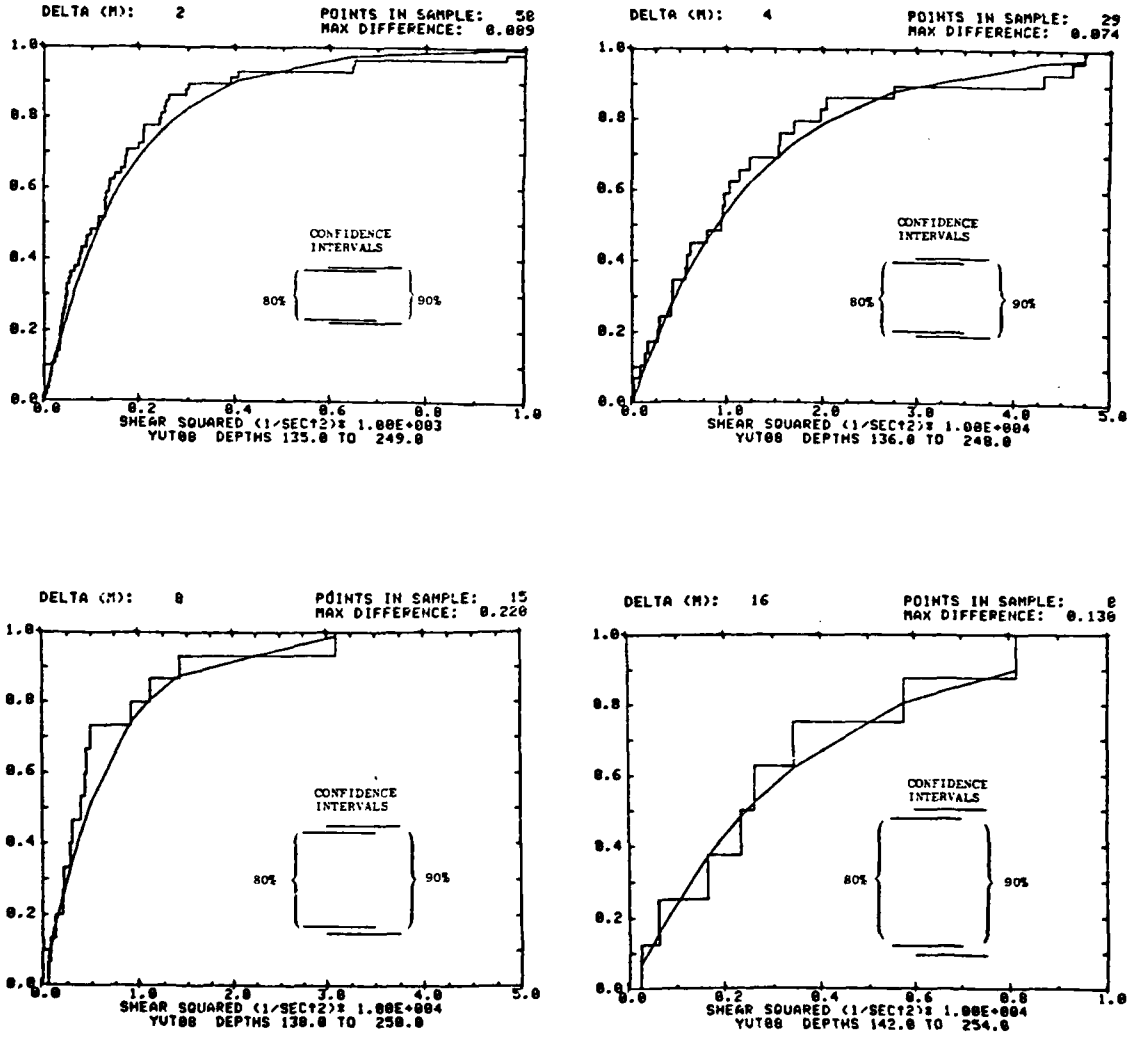

Figure 4.2b Graphical comparison between observed probability of S^2 (step function) and hypothesized χ^2-distribution (smooth function) based on the UT of YVETTE 08. Test statistic is the maximum vertical distance between curves.

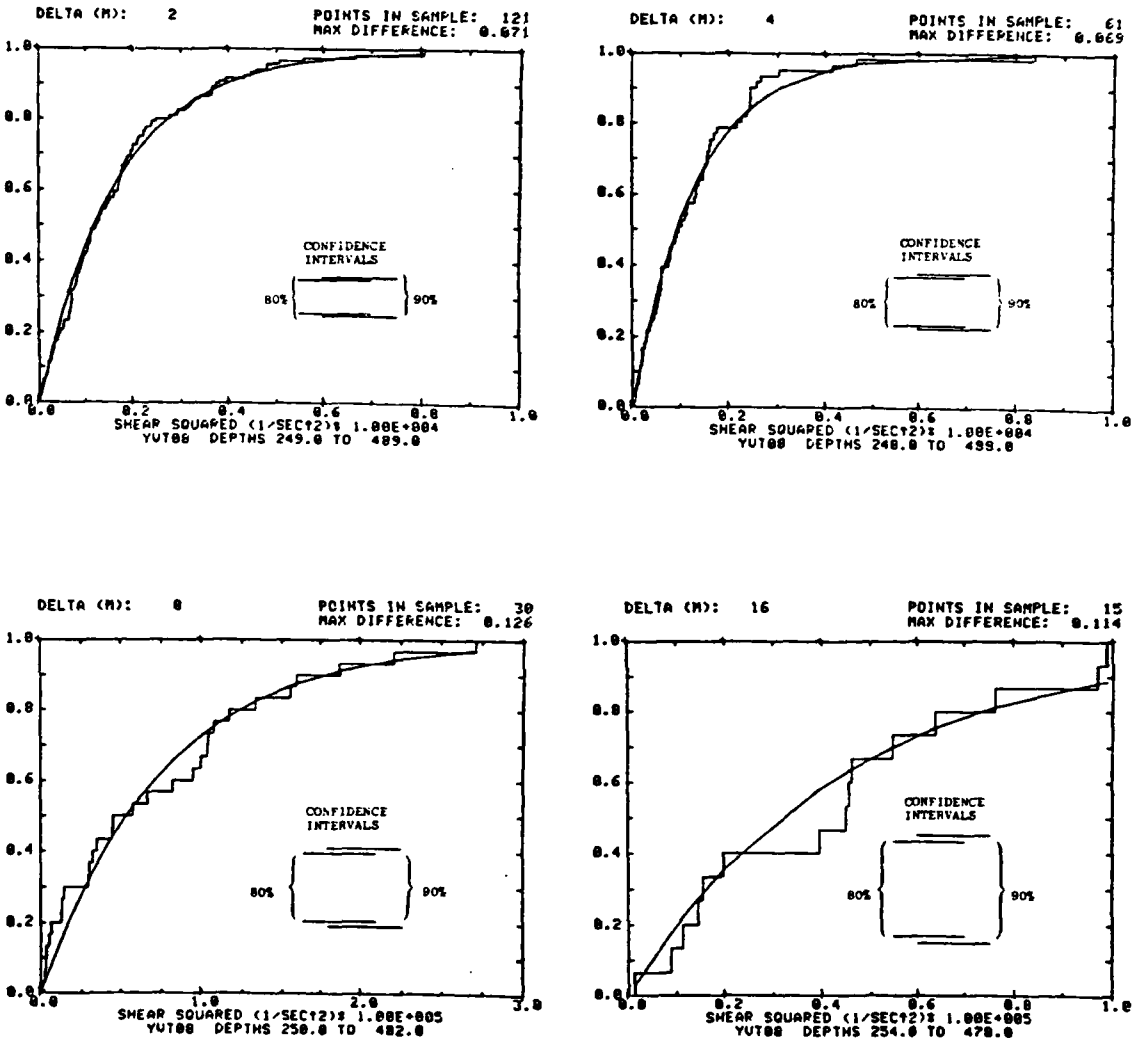

Figure 4.2c Graphical comparison between observed probability of S^2 (step function) and hypothesized χ^2-distribution (smooth function) based on the DL of YVETTE 08. Test statistic is the maximum vertical distance between curves.

Only four stations could divided into three depth regimes. In the other eleven the mixed layer was not well established. In some cases, the layer was so thin that shear values calculated over 8m and/or 16m produced only 4 or 5 values. The test was not applied to samples with fewer than 6 elements. Table B.2 contains the $\hat{\alpha}$ values calculated for all stations.

A breakdown of these results by depth, separation, and $\hat{\alpha}$ range (Table B.3) shows that over 75% of the samples have a critical level of 0.20 or higher. Correspondingly, the model falls within the 80% confidence interval for 75% of the samples.

The conservative bias of the goodness-of-fit test could have been avoided by using the χ^2 goodness-of-fit test rather than the Kolmogorov test. However, that test has its own set of drawbacks. For one thing, the χ^2 test assumes a sample size large enough that the test statistic is governed by a χ^2 distribution. This is probably not the case for many of the regimes studied here. In contrast, the Kolmogorov test is effective for small sample size. Secondly, the χ^2 test depends on breaking the sample up into bins of arbitrary width and, especially with a small sample, the results are sensitive to bin size. Lastly, quantiles of the χ^2 statistic are not known with a great deal of confidence (Conover, 1980). This can reduce the usefulness of the test. For these reasons we chose to accept the overestimated values predicted by the Kolmogorov test and assume that the errors involved are lower than those inherent in the use of the χ^2 test for small sample size.

4.2 TESTING MODEL ASSUMPTIONS

As we mentioned in Section 3, the reasoning which led to the hypothesis of a χ^2 distribution was based on physical assumptions about the nature of internal wave-induced shear. We can apply another set of statistical tests to the distributions of $\Delta_z u$ and $\Delta_z v$ in order to test how well these satisfy the assumptions. This second approach provides an independent test of the χ^2 hypothesis.

We have assumed in our model that the velocity difference components meet the following assumptions:

- $\Delta_z u$ and $\Delta_z v$ occur randomly;
- they are distributed normally;
- they are independent quantities;
- they come from identically distributed popuations.

The reasons for these assumptions were discussed in Section 3. In this section we will show the statistical techniques we used to determine how well our samples satisfied them.

4.2.1 Cox and Stuart Trend Test

We did not attempt to assess directly the randomness of the shear component samples. Instead, we tested to see whether or not a trend existed using the Cox and Stuart Test. A sequence of numbers will have a trend if values

later in the sequence are uniformly higher or lower than earlier values. If no such tendency exists, then the sample is probably made up of random, independent values.

The Cox and Stuart test consists of grouping a sequence of variables, of length n, into pairs (x_i, x_{i+k}), where k=n/2 if n is even and k=(n+1)/2 if n is odd. The pairs are tested to see which value is larger. If we asign a "+" to pairs in which $x_{i+k} > x_i$ and a "-" to pairs in which $x_{i+k} < x_i$, then the test statistic is T, the number of pairs which can be denoted by a "+".* Our null hypothesis is that the probability of observing a "+" is the same as the probability of observing a "-".

The range of acceptance is bounded according to $m-t \leq T \leq t$, where m is the number of pairs excluding ties and t is the greatest number of +'s which would be observed at level $\hat{\alpha}$ based on a probability of 0.5. (See Conover (1980) for the technique for calculating t.) If T falls outside the bounds, then the hypothesis is rejected. The results of this test are shown in Tables B.4 and B.5. Tables B.6 and B.7 show the breakdown by regime, separation, and $\hat{\alpha}$. A total of 91 $\Delta_z u$ profiles and 98 $\Delta_z v$ profiles (out of 114) satisfied the test at $\hat{\alpha} \geq 0.10$. Somewhat more $\Delta_z v$ profiles than $\Delta_z u$ profiles satisified at $\hat{\alpha}$ levels above 0.05, but both types of profiles can definitely be said to be free of trends.

---

* Ties, where $x_{i+k} = x_i$, are disregarded and the total number of pairs is reduced by the number of ties.

4.2.2 Lilliefors Normality Test

In order to evaluate whether the shear component samples come from normal distributions, we applied the Lilliefors test. The test is performed not on an original sequence x_i, but on a normalized sequence.

$$z_i = (x_i - \bar{x}_i)/\lambda^2 \quad i = 1,2,\ldots,n$$

where $\bar{x}_i$ is the sample mean and λ^2 the sample variance. The distribution of this normalized sequence is compared against a normal distribution with zero mean and unit variance. If we define F(z) as our hypothesized normal distribution and S(z) as the observed distribution of the adjusted sequence, then the test statistic is the same as for the Kolmogorov Test:

$$T = \sup_z |F(z) - S(z)|.$$

The Kolomogorov tables cannot be used to evaluate this test, however; instead, special quantiles must be used to make a decision.

The critical levels obtained by applying this test to YVETTE stations are shown in Tables B.8, and B.9. The distributions of $\hat{\alpha}$ values are listed in Tables B.10 and B.11. The test results showed that the normality assumption was satisfied by nearly all profiles (95 of the $\Delta_z u$ and 96 of the $\Delta_z v$) at levels above 0.10.

4.2.3 Chi-Square Independence Test

The chi-squared independence test assumes that we have a sample of length N whose elements can be sorted by two criteria. In our application the two criteria are whether a value comes from $\Delta_z u$ or $\Delta_z v$ and which of a number of bins of width ΔS^2 a shear component value fits. If we break the range of shear into C bins, then each observation can only fall into one of 2C categories.

The test statistic is based on the number of entries in each category. We can envision the possible choices as a matrix with 2 rows (one for each shear component) and C columns (one for each shear range bin). Each possible category can be denoted by indices i and j, where i=1 or 2, j=1,2,...., C. The number of observations in each bin can be denoted as O_{ij}. For each row we define:

$$R_i = \sum_{j=1}^{C} O_{ij},$$

and for each column we define:

$$C_j = \sum_{i=1}^{2} O_{ij},$$

If we also define:

$$E_{ij} = R_i \, C_j \, N^{-1}$$

then the test statistic is defined as

$$T = \sum_{i=1}^{2} \sum_{j=1}^{C} (O_{ij}-E_{ij})^2 E_{ij}^{-1}.$$

The assumption in tnis test is that T is governed by a chi-square distribution with (C-1) degrees of freedom.* If T falls below the $\hat{\alpha}$ level quantile then we can accept the hypothesis that an element occurs in row 1, column j independently of an element in row 2, column j and that this is true for all j. For our case this is equivalent to saying that the $\Delta u/\Delta z$ values occur independently of the $\Delta v/\Delta z$ values.

The critical levels obtained by applying this test to YVETTE profiles are listed in Table B.12 and the $\hat{\alpha}$ distribution in Table B.13. Nearly all of the profile pairs (112) satisfied the independence test at $\hat{\alpha}$ levels above 0.10.

This test does not seem subject to the bin-width sensitivity mentioned when discussing the chi-square goodness of fit test. We presume that this is because two observed distributions are being compared with one another rather than one observed distribution with a hypothesized distribution. Nevertheless, the number of bins was never greater than one-half the number of samples, and in most cases was less than one-third.

4.2.4 The Smirnov Identical Distribution Test

The final assumption to be tested is that the two shear components are governed by identical distributions.

---

* Actually with (number of rows-1).(number of columns-1) degrees of freedom. In this application, with only two rows, we find (C-1) degrees of freedom.

The test chosen, the Smirnov test, is of the Kolmogorov - type in which the test statistic is the maximum separation between two observed distributions. If $S_1(x)$ and $S_2(y)$ are empirical distributions of quantities x and y, and $F_1(x)$ and $F_2(y)$ are their (unknown) hypothesized distributions, then we can test the hypothesis $F_1(x) = F_2(y)$ by generating the statistic

$$T = \sup_z |S_1(z) - S_2(z)|$$

for z's in the range of all possible x's and y's. If T is less than the appropriate quantile, then the hypothesis can be accepted at level $\hat{\alpha}$.

Note that $S_1(x)$ and $S_2(y)$ do not have to have the same number of samples in order to apply this test. However, our samples are of equal length.

The critical levels obtained for YVETTE data are listed in Table B.14, and their distribution is listed in Table B.15. Again, nearly all of the profile pairs (113) may confidently be said to come from identical distributions.

4.2.5 Summary of Assumption Tests

The results of these four tests show that we are statistically justified in accepting the hypotheses based on the assumptions; these assumptions, in turn, led to the postulated χ^2 distribution for shear squared. That is, we can assume with a high level of confidence that the shear components, $\Delta_z u$ and $\Delta_z v$, do come from distributions which

are random, normally distributed, mutually independent, and identically distributed. Table 4.1 shows the percentage of each set of samples which have specific minimum critical levels. For example, the Cox-Stuart Test on $\Delta_z u$ was satisfied by 69% of the samples at $\hat{\alpha}>0.20$, and 80% at $\hat{\alpha}>0.10$. These results lead us to believe that:

- the agreement between S^2 distribution and χ^2 distributions based on sample variances is significant, and,

- that because the assumption tests are not biased, we could extend the previous statement to indicate that S^2 values do seem to come from a χ^2 distributed population.

Table 4.1

Percentages of Samples which satisfy assumption tests at three α levels.

Test	α = 0.20	0.10	0.05
Cox-Stuart $\Delta_z u$	69%	80%	87%
Cox-Stuart $\Delta_z v$	75%	86%	93%
Lilliefors $\Delta_z u$	75%	83%	94%
Lilliefors $\Delta_z v$	80%	84%	92%
χ^2 Independence	93%	98%	99%
Smirnov	96%	99%	100%

Section 5
MODEL APPLICATION

Thus far we have described a model for the distribution of shear in several depth regimes of the upper ocean and established a statistical basis for accepting the model. The final question which must be addressed is how to apply the model.

The key parameter in the model is $\hat{\sigma^2}$, the variance of the velocity component differences based on observations. If we can relate this parameter to large scale, more easily observed quantities, then we can develop the S^2 probability distribution that we seek. One parameter which can be obtained with relative ease is N^2, the Brunt-Väisälä frequency at depth in the water column. Since we divided the YVETTE shear profiles into regimes distinguished by changes in N^2, we examined the possibility of obtaining values of $\hat{\sigma^2}$ through some correlation between N^2 and S^2.

Patterson et al. (1981) have analyzed the same YVETTE data that we used and have reached some conclusions about the relationship between N^2 and S^2. They showed that if N^2 and S^2 are computed over 2 m differencing intervals, then the ratio of $\overline{N^2}$ to $\overline{S^2}$ (where the overbar indicates depth averaging as before) varies between 0.5 and 3.3 in the upper thermocline and deeper layers (Figure 5.1).

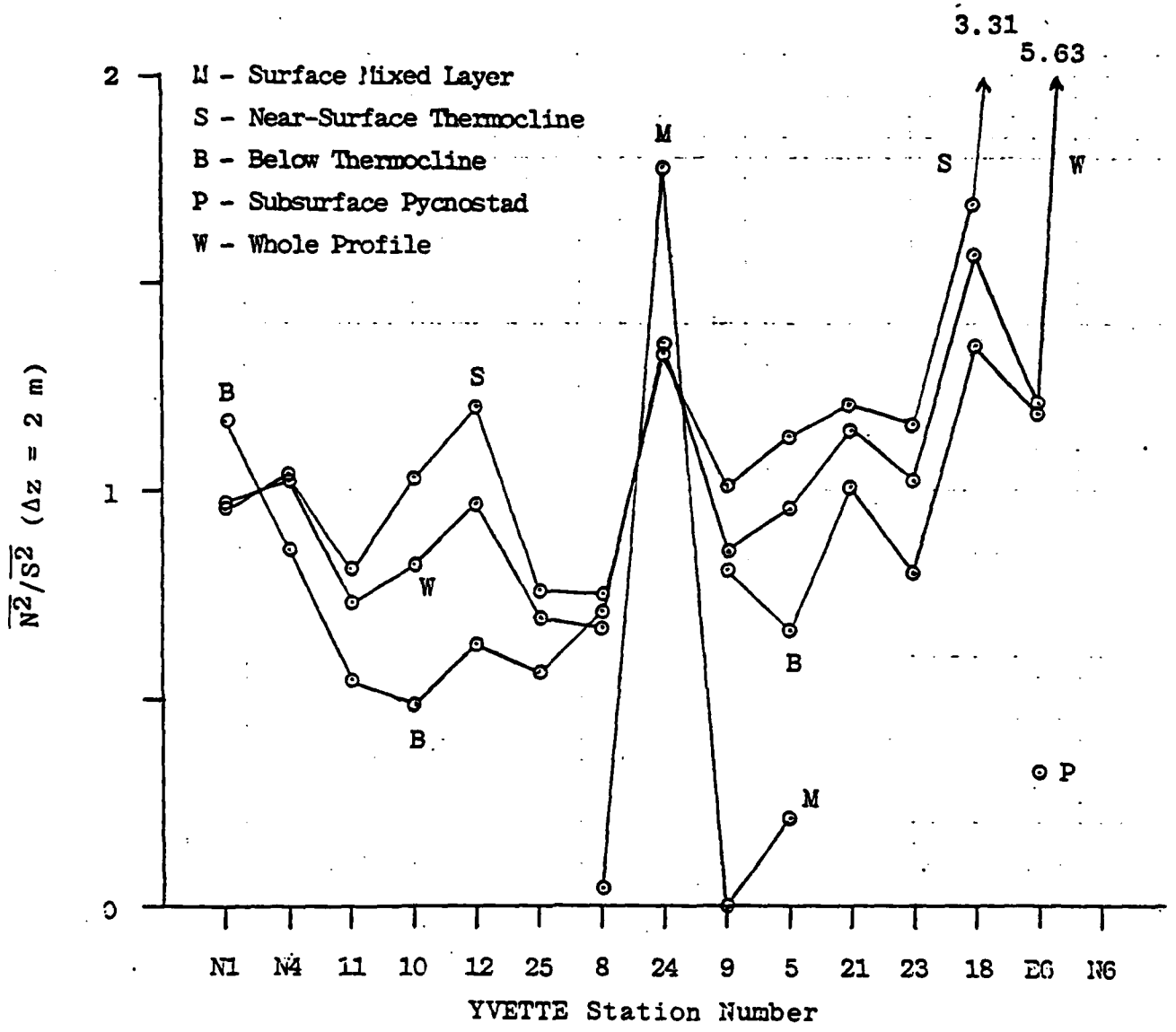

Figure 5.1 Ratio of $\overline{N^2}$ to $\overline{S^2}$ (based on 2 m differencing intervals) versus station number for the different stratification regimes (from Patterson et al., 1981).

The observation that this ratio is reasonably well-behaved motivated us to estimate μ_{S^2} as

$$\mu_{S^2} = k\,\overline{N^2}. \tag{5.1}$$

where k is an order unity proportionality constant. We chose a value of k=1 as a first approximation. We then estimated the sample component variance from (3.6b) as

$$\hat{\sigma}^2 = \tfrac{1}{2}\,\overline{N^2} \quad . \tag{5.2}$$

We tested the performance of the χ^2 model based on (5.2) by repeating the Kolmogorov goodness-of-fit test for ten of the YVETTE stations. The values of the test statistics, $\underline{T}$, are shown in Table 5.1, along with the statistics, $T_{0.201}$ which is the maximum $\underline{T}$ value which would have resulted in a fit at level of significance $\hat{\alpha} = 0.20$. If we had been testing a hypothesis of the form

Ho = "S^2 occur according to a χ^2 -distribution with variance given by (5.2),"

then these results would not be very impressive. Only 6 out of 20 profiles produced $\underline{T}$ values sufficient to result in acceptance at a comfortably high significance level of $\hat{\alpha} \geq 0.20$. On the other hand, the largest calculated T in Table 5.1 is 0.284. The quantity T is defined as the maximum difference between the observed probability distribution and the χ^2 distribution. Thus the model-predicted probability of occurrence (expressed as percentage of occurrence) of S^2 values less than specified levels differed from the

Table 5.1

Test Statistics for the Kolmogorov Test. Test statistics, $\underline{T}$, obtained by estimating $\chi^2(S^2; \hat{\sigma}_S^2$ based on (5.2). The calculations were only carried out for Δz=2 m. $T_{0.20}$ is the statistic which would specify rejection at level 0.20.

STATION	REGIME	$\underline{T}$	$T_{0.20}$
YVETTE 05	UT	0.284	0.151
	DL	0.114	0.081
08	UT	0.065	0.138
	DL	0.174	0.096
09	UT	0.079	0.102
	DL	0.114	0.102
10	UT	0.062	0.126
	DL	0.261	0.084
11	UT	0.161	0.130
	DL	0.183	0.084
12	UT	0.178	0.139
	DL	0.190	0.079
18	UT	0.231	0.111
	DL	0.182	0.091
21	UT	0.183	0.098
	DL	0.075	0.103
23	UT	0.138	0.145
	DL	0.145	0.078
24	UT	0.260	0.187
	DL	0.262	0.296

observed probability by no more than 30% in any of the profiles tested. And in 75% of the cases the difference was less than 20%. These figures serve to indicate the degree of confidence that the user can place in predictions from the statistical model used in this manner.

Section 6
SUMMARY

We have described a statistical model for the distribution of S^2 values in different depth regimes in the upper ocean. The model indicates that a χ^2 distribution with variance computed from the average S^2 in the sample is a good approximation to the observed distribution. The model is physically reasonable and has been verified by statistical analysis of shear profiles measured at 15 different YVETTE stations.

The key to translating this model into a useful tool for future study lies in developing a method of estimating the mean value of S^2, μS^2, in a depth regime from easily measured oceanic parameters. A simple test, based on results of an independent analysis of YVETTE data, consisted of estimating $\mu\hat{S}^2$ from the mean Brunt-Väisälä frequency in the regime. This test showed that such a simplified approach to using the statistical model could yield a cumulative shear distribution which agreed with the observed distribution to 30% or better. This particular use of the model is restricted at present to shear values obtained from differences over two meters.

The reasonable success of the χ^2 model when combined with a fairly primitive scheme for estimating the parameter needed by the model leads us to suggest further study. This would include examination of more S^2 data sets, both vertical profiles and time series from vertically spaced current meters. We would also need

to examine more extensively the nature of the $\overline{N^2}$-$\overline{S^2}$ relationship over various vertical scales. In particular, it appears (Patterson et al., 1981) that the relationship between $\overline{N^2}$ and $\overline{S^2}$ may be less well defined at larger separations. This would of course, reduce the effectiveness of the model over these scales.

APPENDIX A
HYPOTHESIS TESTING

It is possible to employ statistical tests to quantify the degree of confidence which can be assigned to a hypothesis such as "S^2 comes from a χ^2 distribution". To do this we establish a null hypothesis, H_o, regarding some characteristic of the data set being examined:

H_o = "the hypothesis being tested is true."

We then use the data to produce a test statistic, $\underline{T}$, whose value will allow us to either reject or not reject H_o. Notice the choice of words in the last sentence. If we reject H_o, we are in effect stating "the hypothesis is false." But if we do not reject H_o we are not saying "the hypothesis is true." Instead, we are saying "the hypothesis cannot be proven false." We must allow for the possibility that a larger sample might lead us to reject H_o. Tests of this type are rejection tests in that we can only reject or not reject, but never accept H_o without reservation. It is conceivable, for example, that, based on the analysis of a single data set, two mutually exclusive hypotheses could both fail to be rejected. A detailed description of hypothesis testing techniques is presented by Conover (1980). We present an outline here.

Hypothesis testing is subject to two types of error:

- rejecting H_o when H_o is actually true (Type I error), and

- accepting H_0 when H_0 is actually false (Type II error).

We can quantify approximate probabilities of making these errors based on a given sample. We define α, the level of significance, as the maximum probability of making a Type I error, and β as the probability of making a Type II error.

We want both α and β to be as small as possible. Unfortunately, for a fixed sample size, decreases in α are usually accompanied by undesirable increases in β. That is, if we set up a test which tends to minimize the probability of rejecting a true null hypothesis, we increase the chance of accepting a false null hypothesis. The only way to reduce both α and β is to increase the sample size (until eventually the sample encompasses all members of the population being studied and all tests are exact). Only if there is a simple alternative hypothesis to H_0 can β be estimated. This is not the case in general.

The rationale behind the level of significance can be illustrated by a simple example. Suppose we have a finite sample of n random independent observations of some quantity x from which we compute a given estimator $\underline{T}$. We have reason to believe that the true value T (given infinitely many observations) of the parameter being estimated is T_0. Thus our hypothesis H_0 is $T=T_0$. Even if $T=T_0$, the sample value $\underline{T}$ will not equal T_0. We assume that a sample value $\underline{T}$ has a probability density distribution $B(\underline{T})$; then we can use this distribution to estimate the probability of observing any value of $\underline{T}$ given that H_0 is true.

Figure A-1 shows a schematic probability density which assumes $T=T_o$. The test statistic from a single test, $\underline{T}_1$, falls some distance from T_o. If T_1 is so far from T_o that its probability of occurrence is very small, we decide that H_o should be rejected. In order to establish criteria for our decision we decide on upper and lower limits $\underline{T}_{\alpha/2}$ and $\underline{T}_{1-\alpha/2}$, which define a region of acceptance. These $\underline{T}_{\frac{1}{2}\alpha}$ are chosen such that the probabilities of values from the distribution falling beyong these limits are

$$\text{Prob } (\underline{T} \leq \underline{T}_{1-\frac{1}{2}\alpha}) = \tfrac{1}{2}\alpha \qquad \text{(A.1a)}$$

and

$$\text{Prob } (\underline{T} \geq \underline{T}_{\frac{1}{2}\alpha}) = \tfrac{1}{2}\alpha. \qquad \text{(A.1b)}$$

Thus the probability of $\underline{T}$ falling outside the range defined by these limits is α. We set α small; then if we do observe such a $\underline{T}$ we can be confident that we have only a low probability of being wrong by rejecting H_o. α is called the "level of significance" of the test and the range of $\underline{T}$ for which the hypothesis will be rejected is called the "region of rejection." If H_o is true, the chance that $\underline{T}_1$ will fall in the range of rejection is just α; thus α is the probability of rejecting a true null hypothesis (Type I error).

We can also define a second quantity, $\hat{\alpha}$, which we refer to as the critical level of significance. This is defined as the smallest significance level at which the hypothesis would be rejected for a given observation. This is defined by

$$\text{Prob } (\underline{T} \geq \underline{T}_1) = \hat{\alpha}/2 \quad , \qquad \text{(A.2)}$$

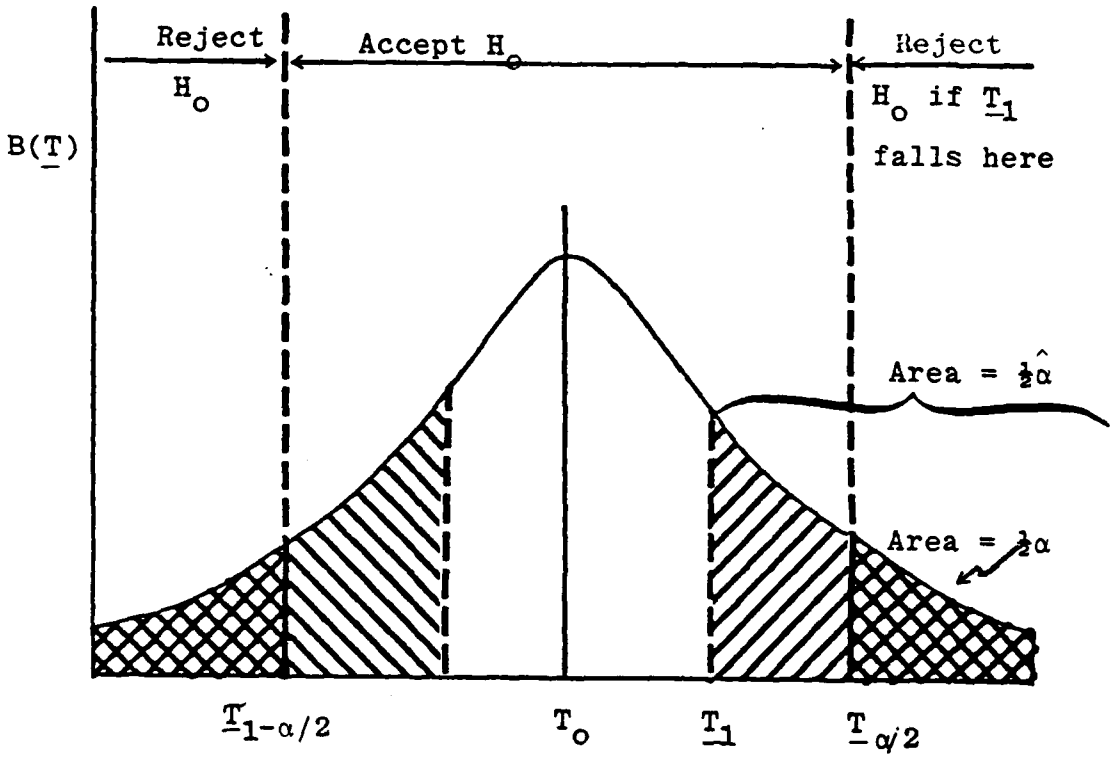

Figure A.1 Schematic probability density of T. The double cross-hatching indicates the area of rejection defined by α. The single- and double-cross-hatching together indicate the critical area defined by $\hat{\alpha}$.

if $\underline{T}_1 > \underline{T}_o$, and a similar definition if $\underline{T}_1 < \underline{T}_o$. This level is also illustrated in the figure. If, as illustrated, $\hat{\alpha} > \alpha$, we have the situation in which the level of significance criterion is more than satisfied. Thus $\hat{\alpha}$ can be looked at as a measure of the robustness of the test. As $\hat{\alpha}$ increases, the confidence with which we can decide not to reject H_o increases.

It is important to notice that α is arbitrarily defined by the tester, while $\hat{\alpha}$ is defined by the sample being tested. We can require that the test be satisfied at some small level α. If we do this, we are taking the point of view that the sample must have every reasonable opportunity to pass the test and that we want to minimize our chances of rejecting a true H_o. Or we can let the sample indicate how well or poorly it satisifes the test by means of $\hat{\alpha}$. This way, our point of view is that we are less concerned with the possibility of rejecting a true hypothesis than we are with assessing the certainty with which we make decisions. We choose to use $\hat{\alpha}$ in our analysis.

APPENDIX B

STATISTICAL RESULTS BASED ON TESTS OF YVETTE DATA

Table B.1

Quantiles of the Kolmogorov Test Statistic*.

Two-Sided Test $p = .80$	.90	.95	.98	.99		$p = .80$	.90	.95	.98	.99
$n = 1$	.900	.950	.975	.990	.995	$n = 21$	.226	.259	.287	.321	.344
2	.684	.776	.842	.900	.929	22	.221	.253	.281	.314	.337
3	.565	.636	.708	.785	.829	23	.216	.247	.275	.307	.330
4	.493	.565	.624	.689	.734	24	.212	.242	.269	.301	.323
5	.447	.509	.563	.627	.669	25	.208	.238	.264	.295	.317
6	.410	.468	.519	.577	.617	26	.204	.233	.259	.290	.311
7	.381	.436	.483	.538	.576	27	.200	.229	.254	.284	.305
8	.358	.410	.454	.507	.542	28	.197	.225	.250	.279	.300
9	.339	.387	.430	.480	.513	29	.193	.221	.246	.275	.295
10	.323	.369	.409	.457	.489	30	.190	.218	.242	.270	.290
11	.308	.352	.391	.437	.468	31	.187	.214	.238	.266	.285
12	.296	.338	.375	.419	.449	32	.184	.211	.234	.262	.281
13	.285	.325	.361	.404	.432	33	.182	.208	.231	.258	.277
14	.275	.314	.349	.390	.418	34	.179	.205	.227	.254	.273
15	.266	.304	.338	.377	.404	35	.177	.202	.224	.251	.269
16	.258	.295	.327	.366	.392	36	.174	.199	.221	.247	.265
17	.250	.286	.318	.355	.381	37	.172	.196	.218	.244	.262
18	.244	.279	.309	.346	.371	38	.170	.194	.215	.241	.258
19	.237	.271	.301	.337	.361	39	.168	.191	.213	.238	.255
20	.232	.265	.294	.329	.352	40	.165	.189	.210	.235	.252
				Approximation for $n > 40$			$\frac{1.07}{\sqrt{n}}$	$\frac{1.22}{\sqrt{n}}$	$\frac{1.36}{\sqrt{n}}$	$\frac{1.52}{\sqrt{n}}$	$\frac{1.63}{\sqrt{n}}$

The entries in this table are selected quantiles of the Kolmogorov test statistics $\underline{T}$. Reject H_o at the level α if $\underline{T}$ exceeds the $1-\alpha$ quantile given in this table. These quantiles are exact for $n \leq 40$. The other quantiles are approximations that are equal to the exact quantiles in most cases. A better approximation for $n > 40$ results if $(n+\sqrt{n/10})^{\frac{1}{2}}$ is used instead of $\sqrt{n}$ in the denominator.

Table B.2

Kolmogorov Goodness-of-Fit Test Results

Critical levels* for the three depth regimes for all 15 YVETTE stations.

Depth Regime =	ML				UT				DL			
Separation =	2m	4	8	16	2	4	8	16	2	4	8	16
Station												
05	<0.01	0.20	--	--	<0.01		0.02	0.20	0.20	0.20	0.10	0.20
08	0.20	0.20	0.20	0.20	0.20	0.20	0.20	0.20	0.20	0.20	0.20	0.20
09	0.20	0.20	0.01	--	0.20	0.10	0.10	0.20	0.20	0.20	0.20	0.20
10	--	--	--	--	0.20	0.20	0.20	0.20	0.20	0.20	0.05	0.10
11	--	--	--	--	0.02	0.20	0.20	0.20	0.20	0.20	0.20	0.20
12	--	--	--	--	0.20	0.20	0.20	0.20	0.20	0.20	0.20	0.20
18	--	--	--	--	0.20	0.20	0.20	0.20	0.20	0.20	0.20	0.20
21	--	--	--	--	0.01	0.02	0.05	0.20	<0.01	0.20	0.20	0.20
23	--	--	--	--	0.20	0.20	0.20	0.20	<0.01	<0.01	<0.01	0.02
24	--	--	--	--	0.10	0.20	--	--	0.20	0.05	--	--
25	--	--	--	--	0.20	0.20	0.20	0.20	0.20	0.20	0.20	0.20
NOR1					0.20	0.20	--	--	0.05	0.20	0.02	--
NOR4	--	--	--	--	0.20	--	--	--	0.20	0.20	0.20	--
NOR6	--	--	--	--	<0.01	<0.01	<0.05	0.20	--	--	--	--
EPOCS6	0.10	0.20	--	--	0.20	0.20	0.20	0.20	0.02	0.20	0.20	0.20
	4	4	2	1	15	13	12	12	14	14	13	11
	11				52				52			

* $\hat{\alpha}$ values listed are not exact. Table A.1 shows five levels: 0.20, 0.10, 0.05, 0.02, 0.01. The $\hat{\alpha}$ value listed in this table indicates the approximate range of $\hat{\alpha}$. For example, a value of 0.10 implies $0.10 \leq \hat{\alpha} < 0.20$.

Table B.3

Kolmogorov Goodness-of-Fit Test Results

Distribution of critical levels by $\hat{\alpha}$ range for depth regimes and separations from all YVETTE stations.

		$\hat{\alpha} \geq 0.2$	$0.2 > \hat{\alpha} \geq 0.1$	$0.1 > \hat{\alpha} \geq 0.05$	$0.05 > \hat{\alpha} \geq 0.02$	$0.02 > \hat{\alpha} \geq 0.01$	$\hat{\alpha} < 0.01$	TOTAL
ML	Δz = 2m	2	1	0	0	0	1	4
	= 4m	4	0	0	0	0	0	4
	= 8m	1	0	0	0	1	0	2
	= 16m	1	0	0	0	0	0	1
UT	Δz = 2m	10	1	0	1	1	2	15
	= 4m	10	1	0	1	1	0	13
	= 8m	9	1	2	0	0	0	12
	= 16m	12	0	0	0	0	0	12
DL	Δz = 2m	10	0	1	1	0	2	14
	= 4m	12	0	1	0	0	1	14
	= 8m	9	1	1	1	0	1	13
	= 16m	9	1	0	1	0	0	11
TOTAL		89	6	5	5	3	7	115

Table B.4

Cox-Stuart Trend Test Results

Critical levels for the $\Delta_z u$ distributions for all YVETTE stations.

DEPTH REGIME =		ML				UT				DL			
SEPARATION =		2	4	8	16	2	4	8	16	2	4	8	16
YVETTE	05	0.20	0.10	--	--	0.20	0.20	0.10	--	0.20	0.20	0.20	0.20
	08	0.20	0.01	0.20	0.10	<0.01	0.05	0.01	0.05	0.20	0.20	0.20	0.10
	09	0.20	0.05	0.20	--	0.20	0.20	0.20	0.20	0.20	0.20	0.20	0.20
	10	--	--	--	--	0.01	<0.01	0.10	0.05	<0.01	<0.01	0.02	0.02
	11	--	--	--	--	<0.01	0.05	0.05	0.02	0.02	0.20	0.10	0.20
	12	--	--	--	--	0.20	0.20	0.20	0.20	0.20	0.20	0.20	0.20
	18	--	--	--	--	0.20	0.20	0.20	0.20	0.02	0.20	0.20	0.20
	21	--	--	--	--	<0.01	0.20	0.10	0.20	0.10	0.20	0.20	0.20
	23	--	--	--	--	0.20	0.05	0.20	0.20	0.20	0.20	0.20	0.20
	24	--	--	--	--	0.10	0.20	--	--	0.20	0.20	--	--
	25	--	--	--	--	0.20	0.20	0.20	0.10	0.20	0.20	0.20	0.20
NOR	1	--	--	--	--	0.20	0.20	--	--	0.20	0.20	0.20	--
	4	--	--	--	--	0.10	--	--	--	0.20	0.20	--	--
	6	--	--	--	--	0.20	0.05	0.20	0.20	--	--	--	--
EPOCS	6	0.20	0.10	--	--	0.20	0.20	0.20	0.20	0.01	0.20	0.20	0.20

Table B.5

Cox-Stuart Trend Test Results

Critical levels for the $\Delta_z v$ distributions for all YVETTE

DEPTH REGIME =		ML				UT				DL			
SEPARATION =		2	4	8	16	2	4	8	16	2	4	8	16
YVETTE	05	0.20	0.10	--	--	0.20	0.20	0.05	--	0.20	0.20	0.20	0.20
	08	0.05	0.20	0.10	0.20	0.20	0.20	0.20	0.05	0.20	0.20	0.20	0.10
	09	0.20	0.20	0.20	--	0.20	0.20	0.10	0.20	0.20	0.20	0.20	0.20
	10	--	--	--	--	0.05	0.20	0.10	0.20	0.20	0.20	0.20	0.20
	11	--	--	--	--	0.20	0.20	0.20	0.20	0.20	0.20	0.20	0.20
	12	--	--	--	--	0.10	0.20	0.20	0.02	<0.01	0.10	0.10	0.05
	18	--	--	--	--	0.20	0.20	0.20	0.10	0.20	0.20	0.20	0.20
	21	--	--	--	--	0.20	0.20	0.20	0.20	0.20	0.20	0.20	0.20
	23	--	--	--	--	0.20	0.20	0.20	0.02	0.20	0.20	0.20	0.20
	24	--	--	--	--	0.20	0.20	--	--	0.20	0.02	--	--
	25	--	--	--	--	0.20	0.05	0.20	0.10	0.20	0.20	0.20	0.20
NOR	1	--	--	--	--	0.20	0.02	--	--	0.02	0.20	0.20	--
	4	--	--	--	--	0.10	--	--	--	0.20	0.20	--	--
	6	--	--	--	--	0.20	0.20	0.20	0.20	--	--	--	--
EPOCS	6	0.20	0.10	--	--	<0.01	0.05	0.05	0.02	0.20	0.20	0.20	0.20

Table B.6

Cox-Stuart Trend Test Results

Distribution of critical levels for $\Delta_z u$ by $\hat{\alpha}$ range for depth regimes and separations for all YVETTE stations.

		$\hat{\alpha} \geq 0.20$	$0.20 > \hat{\alpha} \geq 0.10$	$0.10 > \hat{\alpha} \geq 0.05$	$0.05 > \hat{\alpha} \geq 0.02$	$0.02 > \hat{\alpha} \geq 0.01$	$\hat{\alpha} < 0.01$	TOTAL
	$\Delta z=2$	4	0	0	0	0	0	4
	4	0	2	1	0	1	0	4
ML	8	2	0	0	0	0	0	2
	16	0	1	0	0	0	0	1
	$\Delta z=2$	9	2	0	0	1	3	15
UT	4	9	0	4	0	0	1	14
	8	7	3	1	0	1	0	12
	16	7	1	2	1	0	0	11
	$\Delta z=2$	9	1	0	2	1	1	14
DL	4	13	0	0	0	0	1	14
	8	10	1	0	1	0	0	12
	16	9	1	0	1	0	0	11
TOTAL		79	12	8	5	4	6	114

Table B.7

Cox-Stuart Trend Test Results

Distribution of critical levels for $\Delta_z u$ by $\hat{\alpha}$ range for depth regimes and separations for all YVETTE stations.

		$\hat{\alpha} \geq 0.20$	$0.20 > \hat{\alpha} \geq 0.10$	$0.10 > \hat{\alpha} \geq 0.05$	$0.05 > \hat{\alpha} \geq 0.02$	$0.02 > \hat{\alpha} \geq 0.01$	$\hat{\alpha} < 0.01$	TOTAL
ML	$\Delta z=2$	3	0	1	0	0	0	4
	4	2	2	0	0	0	0	4
	8	1	1	0	0	0	0	2
	16	1	0	0	0	0	0	1
UT	$\Delta z=2$	11	2	1	0	0	1	15
	4	11	0	2	1	0	0	14
	8	8	2	2	0	0	0	12
	16	5	2	1	3	0	0	11
DL	$\Delta z=2$	12	0	0	1	0	1	14
	4	12	1	0	1	0	0	14
	8	11	1	0	0	0	0	12
	16	9	1	1	0	0	0	11
TOTAL		86	12	8	6	0	2	114

Table B.8

Lilliefors Normality Test Results

Critical levels for $\Delta_z u$ profiles from all YVETTE stations.

DEPTH REGIME =		ML				UT				DL			
SEPARATION =		2	4	8	16	2	4	8	16	2	4	8	16
YVETTE	05	0.01	<0.01	—	—	0.01	0.01	0.20	—	0.20	0.20	0.20	0.20
	08	0.05	0.01	0.20	0.10	0.05	0.20	0.01	0.05	0.20	0.20	0.20	0.20
	09	0.20	0.10	0.10	—	0.05	0.20	0.20	0.20	0.20	0.20	0.20	0.20
	10	—	—	—	—	0.20	0.20	0.20	0.20	0.20	0.20	0.20	0.20
	11	—	—	—	—	0.10	0.20	0.20	0.20	0.20	0.20	0.20	0.20
	12	—	—	—	—	0.05	0.20	0.20	0.20	0.20	0.20	0.20	0.10
	18	—	—	—	—	0.20	0.20	0.20	0.20	0.20	0.20	0.20	0.20
	21	—	—	—	—	0.05	0.05	0.20	0.20	0.20	0.20	0.05	0.20
	23	—	—	—	—	0.20	0.20	0.20	0.20	<0.01	0.10	0.05	0.20
	24	—	—	—	—	0.10	0.20	—	—	0.20	0.20	—	—
	25	—	—	—	—	0.05	0.20	0.05	0.20	0.20	0.20	0.20	0.20
NOR	1	—	—	—	—	0.20	0.20	—	—	0.20	0.20	0.20	—
	4	—	—	—	—	0.20	—	—	—	0.20	0.20	—	—
	6	—	—	—	—	0.20	0.20	0.10	0.20	—	—	—	—
EPOCS	6	0.20	0.05	—	—	0.20	0.20	0.20	0.20	0.10	0.20	0.20	0.20

Table B.9

Lilliefors Normality Test Results

Critical levels for $\Delta_z u$ profiles from all YVETTE stations.

DEPTH REGIMES =		ML				UT				DL			
SEPARATION =		2	4	8	16	2	4	8	16	2	4	8	16
YVETTE	05	0.01	0.05	--	--	0.02	0.20	0.20	--	0.20	0.20	0.20	0.20
	08	0.20	0.20	0.20	0.10	0.20	0.20	0.20	0.01	0.20	0.20	0.20	0.01
	09	0.20	0.20	0.10	--	0.20	0.20	0.20	0.20	0.20	0.20	0.20	0.20
	10	--	--	--	--	0.20	0.20	0.20	0.10	0.20	0.20	<0.01	0.20
	11	--	--	--	--	0.01	0.05	0.20	0.05	0.20	0.20	0.20	0.20
	12	--	--	--	--	0.20	0.20	0.20	0.20	0.20	0.20	0.20	0.20
	18	--	--	--	--	0.20	0.20	0.20	0.05	0.20	0.20	0.20	0.20
	21	--	--	--	--	0.01	0.20	0.20	0.20	0.05	0.20	0.20	0.20
	23	--	--	--	--	0.20	0.20	0.20	0.20	<0.01	0.10	0.20	0.20
	24	--	--	--	--	0.20	0.20	--	--	0.20	0.20	--	--
	25	--	--	--	--	0.20	0.20	0.20	0.20	0.20	0.20	0.20	0.20
NOR	1	--	--	--	--	0.10	0.20	--	--	0.20	0.20	0.20	--
	4	--	--	--	--	0.20	--	--	--	0.20	0.20	--	--
	6	--	--	--	--	<0.01	0.10	0.05	0.20	--	--	--	--
EPOCS	6	0.20	0.20	--	--	<0.05	0.20	0.10	0.20	0.20	0.20	0.20	0.20

Table B.10

Lilliefors Normality Test Results

Distribution of critical levels for $\Delta_z u$ by $\hat{\alpha}$ range for depth regimes and separations for all YVETTE stations.

		$\hat{\alpha} \geq 0.20$	$0.20 > \hat{\alpha} \geq 0.10$	$0.10 > \hat{\alpha} \geq 0.05$	$0.05 > \hat{\alpha} \geq 0.02$	$0.02 > \hat{\alpha} \geq 0.01$	$\hat{\alpha} < 0.01$	TOTAL
	$\Delta z=2$	2	0	1	0	1	0	4
	4	0	1	1	0	1	1	4
ML	8	1	1	0	0	0	0	2
	16	0	1	0	0	0	0	1
	$\Delta z=2$	7	2	5	0	1	0	15
UT	4	12	0	1	0	1	0	14
	8	9	1	1	0	1	0	12
	16	10	0	1	0	0	0	11
	$\Delta z=2$	12	1	0	0	0	1	14
DL	4	13	1	0	0	0	0	14
	8	10	0	2	0	0	0	12
	16	10	1	0	0	0	0	11
TOTAL		86	9	12	0	5	2	114

Table B.11

Lilliefors Normality Test Results

Distribution of critical levels for $\Delta_z v$ by $\hat{\alpha}$ range for depth regimes and separations for all YVETTE stations.

		$\hat{\alpha} \geq 0.20$	$0.20 > \hat{\alpha} \geq 0.10$	$0.10 > \hat{\alpha} \geq 0.05$	$0.05 > \hat{\alpha} \geq 0.02$	$0.02 > \hat{\alpha} \geq 0.01$	$\hat{\alpha} < 0.01$	TOTAL
	$\Delta z=2$	3	0	0	0	1	0	4
	4	3	0	1	0	0	0	4
ML	8	1	0	1	0	0	0	2
	16	0	0	1	0	0	0	1
	$\Delta z=2$	9	1	1	1	2	1	15
UT	4	12	1	1	0	0	0	14
	8	10	1	1	0	0	0	12
	16	7	1	2	0	1	0	11
	$\Delta z=2$	12	0	1	0	0	1	14
DL	4	13	1	0	0	0	0	14
	8	11	0	0	0	0	1	12
	16	10	0	0	0	1	0	11
TOTAL		91	5	9	1	5	3	114

Table B.12

χ^2-Independence Test Results

Critical levels for profiles from all YVETTE stations.

DEPTH REGIME =		ML				UT				DL			
SEPARATION =		2	4	8	16	2	4	8	16	2	4	8	16
YVETTE	05	0.10	0.25	—	—	0.25	0.25	0.25	—	0.25	0.25	0.10	0.25
	08	0.25	0.25	0.25	0.25	0.25	0.25	0.25	0.25	0.25	0.25	0.25	0.25
	09	0.25	0.10	0.25	—	0.25	0.25	0.25	0.25	0.25	0.25	0.25	0.25
	10	—	—	—	—	0.25	0.25	0.25	0.25	0.25	0.25	0.25	0.25
	11	—	—	—	—	0.25	0.25	0.10	0.25	0.25	0.25	0.25	0.25
	12	—	—	—	—	0.25	0.25	0.25	0.25	0.25	0.25	0.25	0.25
	18	—	—	—	—	0.25	0.25	0.25	0.25	0.25	0.25	0.25	0.25
	21	—	—	—	—	0.25	0.25	0.25	0.25	0.25	0.25	0.25	0.25
	23	—	—	—	—	0.25	0.25	0.25	0.25	0.25	0.25	0.25	0.25
	24	—	—	—	—	0.25	0.25	—	—	0.25	0.25	—	—
	25	—	—	—	—	0.10	0.25	0.25	0.25	0.05	0.10	0.25	0.25
NOR	1	—	—	—	—	0.25	0.25	—	—	0.25	0.25	0.25	—
	4	—	—	—	—	0.25	—	—	—	0.02	0.25	—	—
	6	—	—	—	—	0.25	0.25	0.25	0.25	—	—	—	—
EPOCS	6	0.25	0.25	—	—	0.25	0.25	0.25	0.25	0.25	0.25	0.25	0.25

Table B.13

χ^2-Independence Test Results

Distribution of critical levels by $\hat{\alpha}$ range for depth regimes and separations for all YVETTE stations.

		$\hat{\alpha} \geq 0.20$	$0.20 > \hat{\alpha} \geq 0.10$	$0.10 > \hat{\alpha} \geq 0.05$	$0.05 > \hat{\alpha} \geq 0.02$	$0.02 > \hat{\alpha} \geq 0.01$	$\hat{\alpha} < 0.01$	TOTAL
	Δz=2	3	1	0	0	0	0	4
	4	3	1	0	0	0	0	4
ML	8	2	0	0	0	0	0	2
	16	1	0	0	0	0	0	1
	Δz=2	14	1	0	0	0	0	15
UT	4	14	0	0	0	0	0	14
	8	11	1	0	0	0	0	12
	16	11	0	0	0	0	0	11
	Δz=2	12	0	1	1	0	0	14
DL	4	13	1	0	1	0	0	14
	8	11	1	0	0	0	0	12
	16	11	0	0	0	0	0	11
TOTAL		106	6	1	1	0	0	114

Table B.14

Smirnov Identical Distributions Test Results

Critical levels for profiles from all YVETTE stations.

DEPTH REGIME =		ML				UT				DL			
SEPARATIONS =		2	4	8	16	2	4	8	16	2	4	8	16
YVETTE	05	0.05	0.20	—	—	0.20	0.20	0.20	—	0.20	0.20	0.20	0.20
	08	0.20	0.20	0.20	0.20	0.20	0.20	0.10	0.10	0.20	0.20	0.20	0.20
	09	0.20	0.20	0.20	—	0.20	0.20	0.20	0.20	0.20	0.20	0.20	0.20
	10	—	—	—	—	0.20	0.20	0.20	0.20	0.20	0.20	0.20	0.20
	11	—	—	—	—	0.10	0.20	0.20	0.20	0.20	0.20	0.20	0.20
	12	—	—	—	—	0.20	0.20	0.20	0.20	0.20	0.20	0.20	0.20
	18	—	—	—	—	0.20	0.20	0.20	0.20	0.20	0.20	0.20	0.20
	21	—	—	—	—	0.20	0.20	0.20	0.20	0.20	0.20	0.20	0.20
	23	—	—	—	—	0.20	0.20	0.20	0.20	0.20	0.20	0.20	0.20
	24	—	—	—	—	0.20	0.20	—	—	0.20	0.20	—	—
	25	—	—	—	—	0.20	0.20	0.20	0.20	0.20	0.20	0.20	0.20
NOR	1	—	—	—	—	0.20	0.20	—	—	0.20	0.20	0.20	—
	4	—	—	—	—	0.20	—	—	—	0.20	0.20	—	—
	6	—	—	—	—	0.20	0.20	0.10	0.20	—	—	—	—
EPOCS	6	0.20	0.20	—	—	0.20	0.20	0.20	0.20	0.20	0.20	0.20	0.20

Table B.15

Smirnov Identical Distributions Test Results

Distribution of $\hat{\alpha}$ for depth regimes and separations from all YVETTE stations.

		$\hat{\alpha} \geq 0.20$	$0.20 > \hat{\alpha} \geq 0.10$	$0.10 > \hat{\alpha} \geq 0.05$	$0.05 > \hat{\alpha} \geq 0.02$	$0.02 > \hat{\alpha} \geq 0.01$	$\hat{\alpha} < 0.01$	TOTAL
	$\Delta z=2$	3	0	1	0	0	0	4
	4	4	0	0	0	0	0	4
ML	8	2	0	0	0	0	0	2
	16	1	0	0	0	0	0	1
	$\Delta z=2$	14	1	0	0	0	0	15
UT	4	14	0	0	0	0	0	14
	8	10	2	0	0	0	0	12
	16	10	1	0	0	0	0	11
	$\Delta z=2$	14	0	0	0	0	0	14
DL	4	14	0	0	0	0	0	14
	8	12	0	0	0	0	0	12
	16	11	0	0	0	0	0	11
TOTAL		109	4	1	0	0	0	114

REFERENCES

Bendat, J. G. and A. G. Piersol, 1971: Random Data: Analysis and Measurement Procedures, Wiley-Interscience, New York, 407pp.

Bretherton, F. D., 1969: Waves and turbulence in stably stratified fluids, Radio Science, 4, 1279-1287.

Conover, W. J., 1980: Practical Nonparametric Statistics, 2d Edition, Wiley, New York, 493pp.

Evans, D. L., H. T. Rossby, M. Mork, and T. Gytre, 1979: YVETTE-a Free-Fall shear profiler, Deep-Sea Res., 26, 703-718.

Lambert, R. B., Jr., D. L. Evans, and P. J. Hendricks, 1980: Data Report - SCIMP and YVETTE, Progress Report I. Ocean Physics Division Technical Report 80-201-04, Science Applications, Inc., McLean, VA.

Loeve, M., 1960: Probability Theory, 2nd Ed., G. Van Nostrand, Princeton, N.J.

Papoulis, A., 1965: Probability, Random Variables, and Stochastic Processes, McGraw-Hill, New York 583pp.

Patterson, S. L., F. C. Newman, D. M. Rubenstein, and R. B. Lambert, Jr., 1981: Spatial distribution of vertical shear, Ocean Physics Division Final Report SAI-82-294-WA, Science Applications, Inc., McLean, VA.

NORDA DISTRIBUTION LIST FOR

REPORT NO. SAI-82-382-WA

STATISTICAL MODELING OF SHEAR

IN THE UPPER OCEAN

Naval Ocean Research and
Development Activity
Code 100, 110, 300, 320,
330, 340, 350, 360
(one copy each)
NSTL Station, MI 39529

Naval Ocean Research and
Development Activity
Code 540
NSTL Station, MI 39529 (5)

NORDA Liaison Office
800 N. Quincy St., Rm. 502
Arlington, VA 22217 (1)

Office of Naval Research
Code 102C
800 North Quincy Street
Arlington, VA 22217
ATTN: Dr. R. Winokur (1)

Office of Naval Research
Code 103T
800 North Quincy Street
Arlington, VA 22217
ATTN: Dr. S. G. Reid (1)

Office of Naval Research
Code 480
800 North Quincy Street
Arlington, VA 22217
ATTN: Dr. L. Goodman (1)

Commander
Naval Oceanography Command
NSTL Station, MS 39529 (1)

Dr. A. Andreassen
OP-95T
Pentagon
Washington, D.C. 20350 (1)

Chief of Naval Operations
Department of the Navy
OP-952
Washington, D.C. 20350
ATTN: CDR Harlett (2)

CAPT H. E. Marxer
OP-212E
Pentagon
Washington, D.C. 20350 (1)

Commanding Officer
Naval Research Laboratory
Washington, D.C. 20375 (1)

Naval Research Laboratory
Code 4340
Washington, D.C. 20375 (1)

Commanding Officer
Naval Oceanographic Office
NSTL Station, MS 39529 (1)

Naval Oceanographic Office
Code 7004
NSTL Station, MS 39529 (1)

Naval Oceanographic Office
Code 7200
NSTL Station, MS 39529 (1)

Commanding Officer
Naval Ocean Systems Center
San Diego, CA 92152 (1)

Naval Electronics Systems Command
Code 320
Washington, D.C. 20360 (1)

Naval Electronics Systems Command
PME 124
Washington, D.C. 20360 (1)

Dr. W. Welch
TRIDENT Systems Project Office
National Center 3
Room 7W66
Washington, D.C. 20360 (1)

Dr. G. D. Smith
Applied Physics Laboratory
The Johns Hopkins University
Johns Hopkins Road
Laurel, MD 20810 (1)

Dr. L. J. Smith
Applied Physics Laboratory
The Johns Hopkins University
Johns Hopkins Road
Laurel, MD 20810 (1)

Dr. G. E. Merritt
Applied Physics Laboratory
The Johns Hopkins University
Johns Hopkins Road
Laurel, MD 20810 (1)

Dr. H. E. Gilreath
Applied Physics Laboratory
The Johns Hopkins University
Johns Hopkins Road
Laurel, MD 20810 (1)

Dr. R. Hoglund
Office, Assistant Sec. of Navy
Pentagon
Room 4-D745
Washington, D.C. 20350 (1)

Dr. P. A. Selwyn
Strategic Support Projects Office
SP-2023
Department of the Navy
Washington, D.C. 20376 (1)

Dr. Melbourne G. Briscoe
Woods Hole Oceanographic Inst.
Woods Hole, MA 02543

Dr. T. Sanford
University of Washington
Applied Physics Laboratory
1013 NE Fortieth Street
Seattle, WA 98195 (1)

Naval Intelligence Support Center
Code 600
4301 Suitland Road
Washington, D.C. 20390 (1)

Naval Underwater Systems Center
New London Laboratory
Code 60
New London, CT 06320 (1)

Administrative Contracting Officer
Defense Contract Administration Services
Management Area - San Diego
Code S0514A
Bldg. 4, AF Plant 19, 4297 Pacific Hwy.
San Diego, CA 92110 (1)

Director
Naval Research Laboratory
Code 2627
Washington, D.C. 20375 (6)

Defense Technical Information Center
Code S47031
Bldg. 5, Cameron Station
Alexandria, VA 22314 (12)

Office of Naval Research
Code N62887
Western Regional Office
1030 E. Green Street
Pasadena, CA 91106 (1)

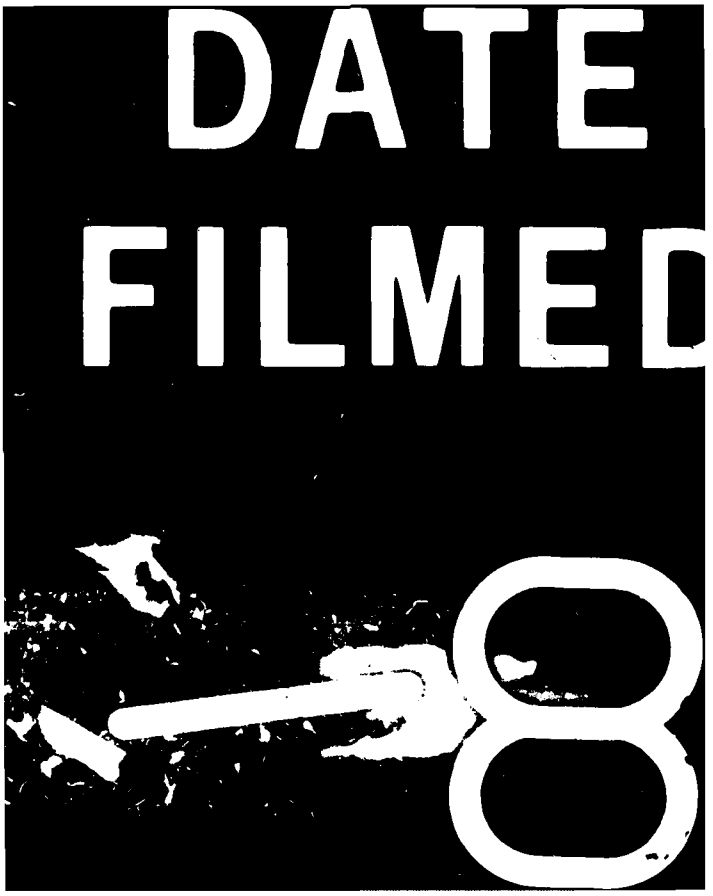
DATE
FILMED
8